Innate Molecular and Cellular Signature in the Skin Preceding Long-Lasting T Cell Responses after Electroporated DNA Vaccination

Lucille Adam, Nicolas Tchitchek, Biliana Todorova, Pierre Rosenbaum, Candie Joly, Candice Poux, Catherine Chapon, Anna-Lena Spetz, Mart Ustav, Roger Le Grand, et al.

Innate molecular and cellular signature in the skin preceding long-lasting T cell responses after electroporated DNA vaccination

Lucille Adam[1], Nicolas Tchitchek[1], Biliana Todorova[1], Pierre Rosenbaum[1], Candie Joly[1], Candice Poux[1], Catherine Chapon[1], Anna-Lena Spetz[2], Mart Ustav[3], Roger Le Grand[1], and Frédéric Martinon[1,*]

[1] CEA – Université Paris Sud 11 – INSERM U1184, Immunology of Viral Infections and Autoimmune Diseases, IDMIT Department, Fontenay-aux-Roses, France.

[2] Stockholm University, Department of Molecular Biosciences, The Wenner-Gren Institute, Stockholm, Sweden.

[3] Institute of Technology, University of Tartu, Tartu, Estonia.

[*] Correspondence Dr. Frédéric Martinon: frederic.martinon@cea.fr

Keywords: DNA vaccine; electroporation; AIM-2; innate response; skin; NHP

Running title: Innate skin DNA-vaccine reponses

Abstract

DNA vaccines delivered with electroporation have shown promising results in pre-clinical models and are evaluated in clinical trials. Here, we aim to characterize early mechanisms occuring in the skin after intradermal injection and electroporation of the auxoGTUmultiSIV DNA vaccine in non-human primates. Firstly, we show that electroporation acts as an adjuvant by enhancing local inflammation, notably via granulocytes, monocytes/macrophages and a $CD1a^{int}$ -expressing cell recruitment. Electroporation also induced Langerhans cell maturation, illustrated by CD86, CD83, and HLA-DR up-regulation, and their migration out of the epidermis. Secondly, we demonstrate the crucial role of the DNA vaccine in the soluble factors release, such as MCP-1 or IL-15. Transcriptomic analysis showed that electroporation played a major role in gene expression changes post-vaccination. However, the DNA vaccine is required to strongly up-regulate several genes involved in inflammatory responses (e.g Saa4), cell migration (e.g *Ccl3*, *Ccl5* or *Cxcl10*), APC activation (e.g *Cd86*) and interferon-inducible genes (e.g *Ifit3*, *Ifit5*, *Irf7*, *Isg15*, or*Mx1)*, illustrating an antiviral response signature. Also, AIM-2, a cytosolic DNA sensor, appeared to be strongly up-regulated, only in the presence of the DNA vaccine and trends to positively correlate with several interferon inducible genes, suggesting the potential role of AIM-2 in the vaccine sensing and the subsequent innate response activation leading to strong adaptive T-cell responses. Overall, these results demonstrate that a combined stimulation of the immune response, in which electroporation and the auxoGTUmultiSIV vaccine triggered different components of the innate immunity, led to strong and persistent cellular recall responses.

Key sentences

- AuxoGTU vaccine and EP triggered different components of the innate immunity.
- AuxoGTU vaccination with EP induce a local release of IL-15 and activation of LC.
- AIM-2 seems to be a sensor of the auxoGTU vaccine.

Grant support

This work was supported by the Agence Nationale de Recherche sur le SIDA et les Hépatites Virales (ANRS, Paris, France), the National Institutes of Health prime award No. 2U19AI057234-06, and ADITEC project funding by the European Commission (grant FP7-HEALTH-2011-280873). It was also supported by the "Programme Investissement d'Avenir" (PIA) managed by the ANR under reference ANR-11-INBS-0008, funding the Infectious Disease Models and Innovative Therapies (IDMIT, Fontenay-aux-Roses, France) infrastructure, the Swedish Research Council, the ANR-10-EQPX-02-01 and funding the FlowCyTech facility (IDMIT, Fontenay-aux-Roses, France). We thank all members of the IDMIT infrastructure for their excellent expertise and outstanding contribution. L.A. held fellowships from Sidaction (Paris, France) and the Fonds Pierre Bergé (Paris, France). N.T. held fellowships from the ANRS (Paris, France).

Abbreviations

Ag, antigen; APC, antigen presenting cell; DC, dendritic cell; EP, electroporation; GTU, gene transport unit; LC, Langerhans cell; M1, type 1 macrophages; M2, type 2 macrophages; MDS, multidimensional scaling; NHP, nonhuman primate; PBS, phosphate-buffered saline; PMN, polymorphonuclear leukocytes; PRR, Pattern Recognition Receptors; TLR, Toll-like receptor.

Introduction

Vaccination is the most attractive strategy to prevent and control infectious diseases (1). However, there are still no effective vaccines against many infectious diseases, including emerging and chronic infections. Modern vaccine strategies have focused on the development of recombinant vectors (2). DNA-based vaccines are an attractive approach (3) to induce immune responses (4–6) by mimicking viral antigen production, including endogenous processing and presentation. (7). The main limitation for the use of DNA vaccines in humans has been their low immunogenicity. To overcome this issue, various approaches have been developed in animal models (Schmaljohn, Spik, and Hooper 2014; Grant-Klein et al. 2012, 2015; Casimiro et al. 2003; Fynan et al. 1993; Cardoso et al. 1996; J B Ulmer et al. 1993; Ferraro et al. 2011; Hutnick et al. 2011) and in humans (13–15). Some of these approaches consist in improving the plasmid vector design to enhance induced immune responses (16–18). Krohn *et al.*, for example, developed an auxoGTU DNA vector that encodes the E2 bovine papillomavirus protein in addition to vaccine antigens (19). The E2 protein facilitates persistence of the plasmid in host cells during cell division (19, 20), leading to a more efficient antigen production over time (19) and a stronger immune response stimulation compared with a conventional CMV plasmid vector (21). Other approaches focused on improving the vaccine delivery into the cells to enhance DNA vaccine efficiency. Electroporation (EP) have notably been developed. Electroporation facilitates the entrance of the DNA vaccine into host cells through short electric impulsions, delivered at the vaccinated site, which temporarily destabilizes the cell membranes (22, 23). This method has dramatically enhanced the immunogenicity of DNA vaccines in non-human primates (NHPs) (24–26) but also in human. Indeed two therapeutic DNA vaccines delivered by the intramuscular route with EP have shown promising results in the context of cervical intraepithelial neoplasia 2/3 patients up to complete regression of lesions in some patients (27, 28).

Another important parameter in the immune response induction is the site of vaccine administration. Indeed several studies highlight the influence of route of immunization in the orientation of immune responses (29, 30). The skin appears to be an attractive organ for vaccination because of the presence, already at steady state, of various subtypes of innate immune cells, including antigen presenting cells (APCs) (31). Indeed, the high density of APCs in the skin is probably related to the lower vaccine doses required for immune responses induction relative to other vaccination routes, providing a cost advantage for vaccines delivered intradermally (32, 33). Langerhans cells (LCs), the unique steady state resident APC population of the epidermis (34, 35), can be mobilized under specific inflammatory conditions (36) and are involved in vaccine responses (37). The dermis is inhabited by several dendritic cell (DC) subsets, which have a distinct capacity to produce cytokines, cross-present antigens, and induce T-cell proliferation and differentiation (38–41). Resident macrophages, the main APC subset of the dermis (42–44), have a key role in homeostasis maintaining (45) and actively participate in the protection against infection by phagocytizing pathogens and secreting soluble factors (46, 47).

Despite the intense use of vaccination, the immune mechanisms that lead to protection are still poorly understood (48). Furthermore, an increasing number of studies suggest that early events are critical for vaccine efficiency (49–51). We previously demonstrated that intradermal auxoGTUmultiHIV DNA vaccination in combination with EP enhances polyfunctional CD4 and CD8 T-cell responses in NHPs (25). We showed that EP affects the localization and intensity of vaccine antigen production in the skin (25, 52) and enhances the LC mobility, facilitating their interaction with vaccine-antigen-expressing cells and their departure from the

112 epidermis (52). Here, we investigated the early cellular and molecular events that occur after
113 intradermal administration of the auxoGTUmultiSIV vaccine combined with EP. We show that
114 this vaccine induced local inflammation, with a recruitment of inflammatory cell population at
115 the vaccinated site. We characterized the soluble factors produced in the local
116 microenvironment and the expression of genes involved in the innate immune response. We
117 highlighted that in these processes EP and the DNA vaccine stimulate different components of
118 the innate immunity that may act in symbioses to induce the strong and persistent T cell
119 responses characteristic of this vaccination strategy.

120

Materials and Methods

Ethical statement and animal housing

Twenty-three adult male cynomolgus macaques (*Macaca fascicularis*) were imported from Mauritius to study early state (9 animals) and adaptive (14 animals) responses. The macaques weighed between 4 and 9 kg. Animals were housed in CEA facilities (accreditation number: B 92-032_02), and handled in accordance with European guidelines for NHP care (EU Directive N 2010/63/EU). The CEA complies with the Standards for Humane Care and Use of Laboratory Animals of the Office for Laboratory Animal Welfare (OLAW, USA) under OLAW Assurance number #A5826-01. This study was approved by the regional committee for the use and care of animals (Comité Régional d'Ethique Ile de France Sud, reference 11_013). Before the beginning of the study, the animals were confirmed to be seronegative for several pathogens (SIV, STLV, filovirus, HBV, herpes B, and measles). Animals were sedated with ketamine (10–20 mg/kg, Imalgene 1000, Rhone-Mérieux, Lyon, France) and 10% of acepromazine (Vtranquil, Ceva Santé Animale, France) during handling.

Vaccination procedure and biopsy sample collection

The DNA auxoGTUmultiSIV vaccine was obtained from FitBiotec (Tampere, Finland). The vaccine was diluted in phosphate-buffered saline (PBS, Gibco Life Technologies, Paisley, UK) to a final concentration of 1 mg/ml. After being shaved, the macaques were immunized with the auxo-GTU-multiSIV plasmid by intradermal injection of 100 µl vaccine formulation or PBS via a 29-gauge needle (Myjector 1ml, Terumo, Leuven, Belgium). Each animal received the DNA vaccine at one site of the skin and the PBS at another to permit paired comparisons of subsequent events immediately followed with an EP performed as previously described (53)

144 Skin biopsies (8 mm in diameter) were performed on anesthetized animals 1, 3, and 8 days after
145 injection.
146
147 *Cell extraction*
148 Cells were extracted from fresh skin specimens using modified versions of published protocols
149 (54, 55). Briefly, the subcutaneous fat tissue was removed and the specimens were then
150 incubated with 4 mg/ml of bacterial protease dispase II (Roche Diagnostic, Meylan, France) in
151 PBS with 1% 100X of penicillin-streptomycin-neomycin (Gibco Life Technologies) and 0.25
152 ug/ml of Fungizone (Amphotericin B, Gibco Life Technologies) for 12 to 16 h at 4°C and then
153 for 40 min at 37°C. Epidermal and dermal sheets were separated and incubated in 2 mg/ml of
154 type D collagenase (Roche Diagnostic, Meylan, France) and 0.2 mg/ml of DNase I from bovine
155 pancreas (Sigma-Aldrich) in RPMI 1640 at 37°C, with shaking, for 20 min and 40 min,
156 respectively. Then, the epidermis was incubated with 0.25X of trypsin (Eurobio, Courtaboeuf,
157 France) for 10 min, the remaining tissue was mechanically dissociated with tweezers, and the
158 cellular suspension obtained was filtrated (100 µm). The dermal tissue was further mechanically
159 dissociated with a gentle MACS dissociator (Miltenyi-Biotec) and the obtained cellular
160 suspension was filtrated (100 µm).
161
162 *Flow cytometry staining and acquisition*
163 Cell mortality was assessed using the LIVE/DEAD Fixable Dead cell stain kit (Life
164 Technologies, Paisley, UK) according to the supplier's instructions. Nonspecific antibody
165 staining was blocked by incubation with a 5% solution of pooled macaque sera. The following
166 monoclonal Abs were used for the characterization of immune cells: HLA–DR (clone L243,
167 Becton-Dickinson - BD), CD1a (clone O10 Dako, Glostrup, Danmark), CD3 (clone SP34-2,
168 BD), CD45 (clone DO58-1283, BD), CD8 (clone RPA-T8, BD), CD20 (clone L27, BD),

CD209 (clone DCN46, BD), CD14 (clone M5E2, BD), CD83 (clone HB15e, BD), CD86 (clone FUN-1, BD), CD163 (clone GHI/61, BD), CD11b (clone Bear 1, Beckman Coulter), CD123 (clone 7G3, BD), CD206 (clone 19.2, BD). CD66abce (clone TET2, Miltenyi-Biotec, Bergisch Gladbach, Germany), CD1c (clone AD5-8E7, Miltenyi-Biotec), and CD207 (clone 2G3, Baylor Institute for Immunology Research, Dallas, TX). Unlabeled Abs were detected with a secondary Ab coupled to an Alexa Fluorochrome, with the Zenon Kit (Life Technologies, Paisley, UK). For the detection of intracellular proteins, cells were incubated in Cytofix/Cytoperm solution (BD) before the staining with Ab diluted in Perm/Wash buffer (BD). Acquisition was performed on a Fortessa cytometer (BD) and the obtained data were analyzed using FlowJo 9.7.1 software (Tree Star, Ashland, OR, USA).

Statistical analysis of flow cytometry data

The percentage of skin cells are represented by the mean ± SD. Data were analyzed using Prism 5.0 (graph-pad Software Inc, La Jolla, CA, USA). The Friedman test with Dunn's post-test was used to assess the significance of differences in cell frequency over time. The Wilcoxon test was used to compare differences in the cell frequency between vaccinated sites and controls.

Luminex measurements

For cytokine analysis, the media of epidermal and dermal cells were obtained by collecting the supernatant during the cell extraction phase and stored at -80°C. Cytokine concentrations were measured using the Milliplex MAP NonHuman Primates Immunoassay kit (Millipore, Guyancourt, France), according to the supplier's instructions. The concentration (in pg/ml) of all 22 tested soluble factors is shown in **Supplementary Table 1 and Supplementary Table**

192 **2**. An ANOVA test with the Bonferroni post-test was used to compare cytokine concentrations
193 between vaccine and PBS injected sites, both with EP.
194
195 *Antigen-specific T cells detected by ELISpot assays*
196 ELISpots were performed using multiScreen 96-well filtration plates (Millipore) prepared as
197 previously described (25). Briefly, the plates were coated by incubation overnight with 10
198 µg/ml monoclonal antibody against monkey IFN-γ (clone GZ-4, Mabtech AB, Sophia
199 Antipolis, France) in PBS at 4°C. Plates were washed with PBS, blocked with culture medium
200 supplemented with 10% heat-inactivated fetal calf serum (FCS, Laboratoires Eurobio; culture
201 medium) and 2×10^5 PBMCs were were added to each well. Fifteen-mer overlapping peptides
202 (11 amino acid overlap), tailored according to the sequence of the MultiSIV protein, were then
203 added in triplicate to a final concentration of 2 µg/ml for each peptide in the culture medium.
204 The peptides were sub-divided into five different sub-pools, covering the sequence of Rev (24
205 peptides), Nef (63 peptides), Tat (29 peptides), and Gag p15/27 (85 peptides). Phorbol 12-
206 myristate 13-acetate (Sigma-Aldrich) and ionomycin (Sigma-Aldrich), at final concentrations
207 of 0.1 and 1 µM, respectively, were used as a positive control. Culture medium alone was used
208 as a negative control. Plates were incubated for 18 h at 37°C in a humid atmosphere containing
209 5% CO_2, washed before an overnight incubation at 4°C with 1 µg/ml biotinylated anti-IFN-γ
210 antibody (clone 7-B6-1, Mabtech AB). Plates were washed again, incubated with 0.25 µg/ml
211 alkaline phosphatase-streptavidin conjugate (Sigma-Aldrich) for 1 h at 37°C before a final
212 washing step. Spots were developed by adding 80 µl of NBT/BCIP substrate (Sigma-Aldrich)
213 to each well and counted with an Automated ELISpot Reader System with KS software (Carl
214 Zeiss, Le Pecq, France). The results are expressed as the mean of IFN-γ spot-forming cells per
215 10^6 PBMCs (IFN-γ SFC/million PBMCs) of triplicate wells. The background was calculated as
216 the mean number of IFN-γ SFC/million PBMCs in non-stimulated samples. Samples yielding

more than 50 IFN-γ SFC/million PBMCs after removal of the background were scored as positive.

RNA extraction and transcriptomic profiling

Whole-skin RNA was extracted from macaque skin biopsies, stored in RNA Later, using Tissue Ruptor® followed by the RNeasy Plus Universal Kit (Qiagen), according to the manufacturer's instructions. The quality of the total RNA was verified using an Agilent 2100 Bioanalyzer. RNA quantity was measured using a NanoDrop ND-1000 Spectrophotometer. Cyanine-3 (Cy3) labeled cRNA was prepared from 200 ng total RNA using the Quick Amp Labeling Kit (Agilent), according to the manufacturer's instructions, followed by RNeasy column purification (QIAGEN, Valencia, CA). Dye incorporation and cRNA yield were measured using a NanoDrop ND-1000 Spectrophotometer. Cy3-labelled cRNA (1.65 µg) was fragmented at 60°C for 30 min in a reaction volume of 55 µL containing 1X Agilent fragmentation buffer and 2X Agilent blocking agent, following the manufacturer's instructions. Upon completion of the fragmentation reaction, 55 µL 2X Agilent hybridization buffer was added to the fragmentation mixture and the mixture hybridized to Agilent Rhesus Macaque Gene Expression Microarrays v2 for 17 h at 65°C in a rotating Agilent hybridization oven. After hybridization, microarrays were washed for 1 min at room temperature with GE Wash Buffer 1 (Agilent) and 1 min at 37°C with GE Wash buffer 2 (Agilent). Slides were scanned immediately after washing on an Agilent DNA Microarray Scanner (G2505C) using a one color scan setting for 4 x 44K array slides (Scan Area 61 x 21.6 mm, scan resolution 5 µm, dye channel set to Green, PMT set to 100%). The scanned images were analyzed with Feature Extraction Software 10.7.3.1 (Agilent) using default parameters.

Transcriptomic analysis

Transcriptomic signals were background corrected using the Robust Multi-array Average (RMA) method and quantile-normalized. Differentially expressed genes were identified using a t-test (p-value<0.01) and a fold-change threshold of 1.5. Functional enrichment analyses of biological functions and upstream regulators were performed using Ingenuity Pathways Analysis software (Ingenuity Systems, Inc.). IPA maps each gene identifier to its corresponding molecule in the Ingenuity Pathways Knowledge Base (IPKB). P-values generated by the Fisher's exact test were adjusted using Benjamini-Hochberg Multiple Testing for all analyses. The multidimensional scaling (MDS) representation was generated using the SVD-MDS algorithm (56). MDS methods aim to represent the similarities and differences among high dimensionality objects in a space with a low number of dimensions, generally 2 or 3, for visualization purposes (57). Pairwise distances between the dots are proportional to the Euclidean distances between the samples. Biological conditions are indicated by convex hulls (*i.e.*, the smallest convex set containing the points). The Kruskal Stress criterion (57), shown in the representation, quantifies the quality of the representation as a fraction of the information lost during the dimensionality reduction procedure.

Data dissemination

Raw transcriptomic data used in this study are available on the EBI ArrayExpress database (http://www.ebi.ac.uk/arrayexpress) under accession number E-MTAB-8973. Microarrays data are also available on the IDMIT data dissemination platform (http://data.idmitcenter.fr/DNAvaccination-EP/).

Results

Systemic immune response induced by auxoGTUmultiSIV DNA vaccine combined with EP

In a previous work, we described the immunogenicity of the auxo-GTUmultiHIV vaccine. We showed that the specific design of this DNA vaccine associated with EP induces a strong and persistent specific recall cellular responses agaisnt the HIV Ag encoding by the palsmid (25). Here we aimed to characterize the innate events at the vaccine injection site to understand the link of these events with the adaptive immune response induction in the context of the auxoGTUmultiSIV vaccine. We first compared the immunogenicity of the auxoGTUmultiSIV vaccine delivered with or without EP in two groups of animals injected intradermally at weeks 0, 4, and 12 (**Figure 1**). We measured specific T-cell responses through the release of IFN-γ by ELISpot in vaccinated animals.

As expected, the EP group showed an enhanced adaptive response relative to the non-EP group. The strongest responses were directed against Nef, followed by Gag, Tat, and Rev. Cumulative measurements showed that the magnitude of the adaptive response was very high after the third immunization, with a persistent vaccine response that lasted at least 30 weeks post first immunization.

Identification of epidermal and dermal APC populations at baseline in macaque skin

To study the effect on skin cells of auxo-GTU DNA vaccine associated with EP, we first characterized immune-cell subsets present in macaque epidermis and dermis at baseline. Epidermal and dermal sheets were enzymatically separated and each skin layer was processed for cytometry analysis. Dead cells, debris, and $CD45^-$ cells were excluded from the analysis to characterize innate immune-cell populations (**Supplementary Figure 1**).

LCs were identified in the epidermis by their high expression of CD1a and HLA–DR. We confirmed our previous finding (34), showing that macaque LCs are negative for CD1c in contrast to human LCs (40, 58) (**Supplementary Figure 1A**).

Few CD66-expressing granulocytes were detected in the dermis at baseline (**Supplementary Figure 1B**). We furthermore detected dermal $CD1a^{+}CD163^{low}$ cells, which could be subdivided into two subsets. The main $CD1a^{+}CD1c^{+}$ subset corresponded to dermal DCs (DDCs), according to previous publications (34, 36). The minor dermal $CD1a^{+}$ subset expressed high levels of CD1a, but not CD1c, a phenotype that closely resembles to LCs, suggesting that they are LCs migrating through the dermis (mLCs). Dermal macrophages were identified based on their expression of CD14 and their high expression of both HLA–DR and CD163.

These analyses identified different APC populations present at baseline in macaque skin. To characterize the cell abundance and phenotype changes occurring over time after auxoGTU DNA vaccination in combination with EP, we then performed a kinetic and extended phenotypical analysis.

Electroporation induces a rapid recruitment of inflammatory cells in both the epidermis and the dermis

To assess cell recruitment after vaccination, skin biopsies were collected at baseline (d0), one (d1), three (d3), and eight days (d8) after PBS and DNA injection combined with EP, (PBS/EP) and (DNA/EP), respectively (**Figure 2**).

311

312 In the epidermis, PBS/EP and DNA/EP induced a significant influx of PMNs at d1 ($p = 0.0008$
313 and $p < 0.0001$, respectively), which declined at d3 ($p = 0.0061$ and $p = 0.0487$, respectively)
314 and a significant influx of $CD14^+HLA\text{-}DR^+$ cells at d1 ($p = 0.0011$ and $p = 0.0008$, respectively)
315 and d3 after PBS/EP ($p = 0.0084$) (**Figure 2A**).

316

317 In the dermis, both PBS/EP and DNA/EP treatment induced an influx of PMNs at d1 ($p =$
318 0.0031 and $p = 0.0061$, respectively) with a significant stronger influx at the DNA/EP site
319 compared with the PBS/EP site ($p \# = 0.0391$). The frequency of PMNs reduced by d3 but was
320 still significantly increased in the PBS/EP group ($p = 0.0370$). We did not observed significant
321 changes compared with the baseline among the CD14+HLA-DR+ subset in the dermis at any
322 time point. (**Figure 2B**).

323

324 These data suggest that EP is the main inducer of the local inflammation following vaccination,
325 with only a slight influence of the DNA vaccine. To confirm this hypothesis, we measured the
326 frequencies of PMNs and CD14+HLA-DR+ cells in the epidermis and dermis in 4 conditions:
327 PBS, PBS/EP, DNA, DNA/EP at d1 and d3 (**Supplementary Figure 2**). In the epidermis, even
328 if not significant probably due to the low number of animal per group (n=3) we confirmed a
329 similar recruitment of PMNs at the PBS/EP and DNA/EP sites while very low increase of this
330 population occurred at the PBS and DNA sites. In the dermis, a stronger recruitment of PMNs
331 at the EP site occurred compared with the non-EP sites. Even if less clear, the same observation
332 could be made for the $CD14^+HLA\text{-}DR^+$ subset.

333

Altogether, these results suggest that EP plays a major role in the early induction of local inflammation, whereas the auxo-GTU DNA vaccine *per se* only influences this process slightly.

Electroporation triggers three subsets of monocytes/macrophages according to their expression levels of CD11b and CD163

We observed an influx of $CD14^+HLA\text{-}DR^+$ cells following vaccination in the epidermis but not in dermis. We decided to further characterize the phenotypes of these cells at baseline and following injection and EP (**Figure 3**). $CD14^+HLA\text{-}DR^+$ cells were completely absent from the epidermis and formed a homogeneous population in the dermis at baseline whereas additional $CD14^+HLA\text{-}DR^+$ phenotypic subsets, based on CD11b and CD163 expression, appeared after PBS/EP and DNA/EP, in each skin sheets.

At baseline, resident macrophages, defined as $CD163^{high}CD11b^+$ (subset 1), were present only in the dermis. After injection and EP, a second subset expressing a higher level of CD11b and a lower level of CD163 compared with resident dermal macrophages, and a third subset $CD11b^+CD163^-$ cells arose (**Figure 3A**). The second and third subsets are likely newly recruited cells because of their total absence in the skin at baseline and their presence in the epidermal and dermal compartments after both PBS/EP and DNA/EP. Indeed, we measured a significant influx of the $CD11b^{high}CD163^{mid}$ subset (subset 2) at d1 ($p = 0.0031$) and d3 ($p = 0.0031$) post-PBS/EP, as well as post-DNA/EP but with significance only at d1 ($p < 0.0001$) (**Figure 3B**). There was also a significant recruitment of the $CD11b^+CD163^-$ subset (subset 3) that peaked at d1 ($p = 0.0014$) post-DNA/EP. However, no changes in the resident dermal macrophage population (subset 1) could be noticed after injection and EP. Since resident macrophages represent the main $CD14^+HLA\text{-}DR^+$ population even after injection and EP it may explains why

only a non-significant trend of increase of this population was measured when considering the globality of the $CD14^+HLADR^+$ subsets (**Figure 2B**).

To further characterize these three $CD14^+HLA\text{-}DR^+$ subsets, we performed additional surface staining by focusing on d1 post DNA/EP condition in the dermis (**Figure 3C**). The resident dermal macrophages (subset 1), were $CD206^+CD40^+CD86^{high}CD11b^+HLA–DR^+$. This phenotype is similar to M2-type macrophages (47, 59). The second subset was instead $CD206^-CD40^-CD86^+HLA–DR^+$, a phenotype closer to M1-type macrophages (60). The third subset also lacked expression of CD206 and showed the lowest expressions of HLA–DR and CD86, suggesting these cells were the least activated. Indeed, this third subset resembles to circulating monocytes (**Supplementary Figure 3B**), suggesting that these cells might be monocytes circulating in the dermis or in a process of differentiation.

Altogether, these results show that EP *per se* induced a rapid recruitment of two additional $CD14^+HLA\text{-}DR^+$ populations to the vaccinated skin, which were distinct from resident macrophages.

Electroporation induces LC activation and the emergence of a newly-recruited $CD1a^{int}$ DC subset in the epidermis

We previously showed that EP enhances LC mobility in the epidermis by *in vivo* microscopy, facilitating the interaction of LCs with antigen-transfected cells (52). Here, we further investigated the effect of the auxoGTUmultiSIV DNA vaccine combined with EP regarding DC subpopulations in the skin.

382

383 At baseline in the epidermis, only the CD1a-expressing LCs could be observed, while two
384 CD1a-expressing subsets were present after PBS/EP and DNA/EP: (i) the first subset
385 expressing the highest level of CD1a and negative for CD1c corresponds to LCs; and (ii) the
386 second subset expressed CD1a at an intermediate level and was positive for CD1c (**Figure 4A**).
387 We studied the dynamics of these two CD1a-expressing cell types over time after vaccination
388 **(Figure 4B)**. We observed a transient increase of LCs frequency at d1 with significance only
389 at the DNA/EP site ($p = 0.0016$). At the same time point, LC strongly up-regulated their
390 expression of CD86, CD83, and HLA-DR compared to the baseline, illustrating their activation
391 (**Figure 4C**). This transient increase was followed by a significant decrease in the LCs
392 frequency between d1 and d3 at both the PBS/EP ($p = 0.0061$) and DNA/EP ($p = 0.0370$) sites,
393 suggesting migration of LCs out of the epidermis. A comparison of the PBS/EP and DNA/EP
394 conditions at d1 and d3 revealed no significant changes in LC frequency due to the presence of
395 the auxoGTU DNA vaccine (**Figure 4B**).

396

397 The $CD1a^{int}CD1c^{+}$ subset appeared in the epidermis at the PBS/EP and DNA/EP injection sites
398 at d1 (DNA/EP $p = 0.0221$) and d3. A comparison of the PBS/EP and DNA/EP conditions
399 showed a significant effect of the auxoGTU DNA vaccine regarding the recruitment of this
400 subset at d1 ($p = 0.0288$) and d3 ($p = 0.0011$) (**Figure 4B**). No staining of CD207 was observed
401 at the surface of the $CD1a^{int}CD1c^{+}$ cells, demonstrating that these cells were distinct from LCs.
402 Nevertheless, approximately 20% of these cells showed a CD207 expression in the intracellular
403 compartment, suggesting they may share some LC characteristics (**Figure 4D**).

404 In the dermis, we did not noticed any effect of the PBS/EP or DNA/EP treatment on DC
405 populations (**Supplementary Figure 4**).

These results demonstrate that EP induced LC activation as defined by increase expression of HLA-DR, CD86 and CD83 at d1. Subsequently, the activated LC might migrate out of the epidermis, illustrating by a LC frequency decrease between d1 and d3. The auxoGTU vaccine seems to have no to little impact in these process but enhance the recruitment of a second CD1a-expressing cell subset that, even if distinct from LCs, may share some LC characteristics.

The AuxoGTU DNA vaccine induces the secretion of soluble factors

Our results suggest that EP is the main inducer of the local cell recruitment with only a slight influence of the auxo-GTU DNA vaccine. We now decided to study the local effect of the vaccination on the molecular microenvironment. We analyzed soluble factors released by epidermal and dermal cells after PBS/EP or DNA/EP treatment using multiplex assays (**Figure 5**).

We observed the release of pro-inflammatory soluble factors by both epidermal and dermal cells such as MCP-1, IL-8, IL-13, and IL-15, at each time point post-injection ex-vivo (**Figure 5**, **Supplementary Table 1, and Supplementary Table 2)**. Interestingly, we observed a clear enhanced release of MCP-1 at d1, IL-15 at d1, d3, and d8 both in the epidermis and dermis, and MIP-1β, IL-18, and TNF-α primarily in the dermis, in the presence of the DNA vaccine. Anti-inflammatory soluble factors, such as IL-10, IL1-RA, and sCD40L, were also upregulated, mainly in the dermis only in the presence of the DNA vaccine. For example, sCD40L levels significantly increased ($p = 0.0306$) at d8 at the DNA/EP injection site, whereas there was no change of this factor at the PBS/EP injection site. Several other soluble factors, such as IL-1β

remained under the detection threshold of the device both in epidermis and dermis over the kinetics (**Supplementary Tables 1 and 2**).

These results highlighted the effect mediated by the auxoGTU DNA vaccine on the initiation of the pro-inflammatory and concomitant balanced anti-inflammatory soluble molecular response induced in the skin during the early phase with this vaccination strategy.

Transcriptomic analyses reveal early immune events that distinguish PBS/EP and DNA/EP responses

To further characterize the molecular events involved in the auxoGTU DNA vaccination strategy combined with EP, we performed a transcriptomic analysis of skin biopsies collected at d1, d3, and d8 after PBS/EP and DNA/EP injections and at an untreated site (baseline) using microarrays (**Figure 6**).

Among the 43,603 genes on the microarrays, 3,963 (9.09%) were differentially expressed in at least one condition relative to baseline. Consistent with the observed early cellular events, the strongest transcriptomic responses were observed at d1 for both PBS/EP and DNA/EP conditions, with 2,655 (6.09%) and 1,131 (2.59%) genes differentially expressed, respectively (**Figure 6A**). **Figure 6B** shows a multidimensional scaling (MDS) representation of transcriptomic profiles calculated based on the list of 3,963 genes differentially expressed in at least one condition. Each dot in the MDS represents a biological sample and the distances between dots are proportional to the transcriptomic distances between the samples. Consistently with the numbers of differentially expressed genes found at each time point, we observed that the PBS/EP and DNA/EP samples from d1 post-injection were displaying the most differential

responses relative to baseline. The PBS/EP and DNA/EP conditions overlapped in the MDS representation at d3 and d8, suggesting similar responses. In contrast, the profiles for the PBS/EP and DNA/EP conditions were non-overlapping at d1, suggesting that different molecular events were involved at the earliest timepoint.

We identified two sets of 1,549 and 1,826 genes. The first set was up-regulated throughout the time course, whereas the second set was down-regulated. Canonical pathway analysis of these gene clusters revealed that up-regulated genes were significantly associated with cyclins and cell-cycle regulation, p38 MAPK signaling, and TREM1 signaling (**Supplementary Figure 4A**). These pathways are involved in cell division, inflammation, and neutrophil and monocyte/macrophage activation, respectively. We also noticed that canonical pathways involved in pattern recognition, acute phase responses signaling, and toll-like receptor signaling were also up-regulated. These pathways are involved in antigen or danger signal recognition. Genes involved in interferon signaling were also strongly upregulated, especially at d1 at the DNA/EP injection site.

The analysis of upstream-regulators (**Supplementary Figure 4B**) showed the up-regulation of *CSF2*, involved in granulocyte and monocyte/macrophage production, differentiation, and function, *ERBB2*, a member of the epidermal growth factor receptor family of receptor tyrosine kinases, and *TNF*, involved in various inflammatory responses. Several genes encoding transcription factors, such as *FOXM1, MYC, TP63,* and the *NFKB* complex, were upregulated, whereas other transcription factor genes, such as *TP53, NUPR1*, and *KDM5B* were downregulated after both PBS/EP and DNA/EP.

The transcriptomic analysis showed that both PBS/EP and DNA/EP vaccination strategies induced the strongest changes in gene expression at d1 post-injection. The changes in gene expression induced by the PBS/EP and DNA/EP injections were associated with cellular division, influx, and activation, as well as immune responses. The strongest differences between the PBS/EP and DNA/EP transcriptomic profiles occurred at d1.

The DNA vaccine up-regulated the expression of several genes associated with cell migration, inflammation and interferon responses

To focus on genes involved in the innate immune response, we next restricted the transcriptome analysis to cytokines/chemokines and their receptors and activation markers differentially expressed relative to baseline (**Figure 7**). We also focused on the transcripts differentially expressed between the DNA/EP and PBS/EP conditions.

Several genes involved in cell migration, such as *CCL3*, *CXCL10, CXCL11*, *CCL1, CCL5, CCL11,* and *IL8* were the most significantly up-regulated, relative to baseline, at both the PBS/EP and DNA/EP injection sites, especially at d1 and d3 (**Figure 7A**). *IL20,* a cytokine produced by keratinocytes during skin inflammation, was also upregulated at d1 and d3 at both the PBS/EP and DNA/EP injection sites. Several genes involved in APC activation, such as *CD80* and *CD86* were significantly up-regulated at d1 and d3, consistently with the phenotypic analyses (**Figure 4C**). Interestingly we noticed a stronger up-regulation of several of these genes in the presence of the DNA vaccine. For example, *IRF7*, a gene encoding the IRF7 transcription factor, involved in virus-inducible cellular genes, was more strongly up-regulated at d1 post DNA/EP than after PBS/EP.

To highlight the specific contribution of the auxoGTU DNA vaccine in the gene perturbation post injection and EP, we performed a comparison of the gene expression profiles between the PBS/EP and DNA/EP at each time point. Only 184 genes were differentially expressed between the PBS/EP and DNA/EP conditions (**Figure 7B)**. Among the up-regulated genes in DNA/EP, we found several interferon-inducible genes, such as *IFIT3*, *IFIT5*, *IRF7*, *ISG15* or *MX1*. Furthermore, we found an up-regulation of serum amyloid A (*SAA4*) and *CCL3*, *CCL5*, *CXCL11*, and *CXCL10,* suggesting that the auxoGTU DNA vaccine significantly affected the expression of several specific genes involved in the immune response and notably in the interferons signaling pathway.

Finally, we assessed which Pattern Recognition Receptors (PRRs) were involved in this DNA vaccine strategy by studying the gene expression of TLRs 1 to 10 and adaptor molecules (**Figure 8A**). Surprisingly, we observed an up-regulation of the *TLR2* and the *TLR3* at d1 post DNA/EP, while no change occurred in the expression of *TLR9*, able to recognize unmethylated CpG motifs contained in plasmid DNA. The contribution of TLR9 in DNA vaccine sensing is a matter of debate and some studies have shown that TLR9 is dispensable in vaccine plasmid sensing, suggesting the contribution of other DNA sensors. We examined the transcription of cytosolic DNA sensors and observed the highly significant up-regulation of *AIM-2* at d1 only at the DNA/EP injection site (**Figure 8B**). Upon binding to dsDNA, AIM-2 forms the inflammasome, leading to the cleavage of pro-interleukin 1β and 18 by caspase 1 and the secretion of their active forms. AIM-2 is involved in DNA sensing inflammasome but other inflammasome structure can be formed involving notably NOD-like receptor as NLRP3 and NLRP4. We did not observed enhanced expression of *NLRP3* or *NLRP4* but we highlighted a significant increase of *CASP1*, the gene coding the caspase1 only at d1 post DNA/EP (**Figure**

525 **8C**). These data suggest a specific activation of the DNA sensing inflammasome involving
526 AIM-2.

527

528 It has been recently demonstrated that AIM-2 is an essential sensor for the immunogenicity of
529 DNA vaccines in mice (61). Indeed we observed a trend of positive correlation between the
530 relative AIM-2 expression and several interferon inducible gene expression at d1 post DNA/EP
531 (**Figure 8D**). Even if not significant, probably due to a fewer number of individuals in this
532 analyze, these trends suggested a link between the auxoGTU DNA vaccine sensing via AIM-2
533 and the enhancement of immune system activation.

534

535 Overall, these results demonstrate that the DNA/EP vaccination strategy affected cell division,
536 cell migration, and cellular activation. In addition, even if the EP is able to induce gene
537 expression change, the auxoGTU DNA vaccine is required to strongly enhance these changes.
538 Indeed, the DNA vaccine specifically enhanced the expression of *AIM-2*, a DNA sensor
539 involved in inflammasome formation and subsequent innate inflammatory responses.

540

541

Discussion

Innate immunity has been shown to play a key role in the orientation of adaptive immune responses (50, 51, 62), suggesting its impact on vaccine efficiency (48). We have previously shown that auxo-GTUmultiHIV DNA vaccination delivered with EP induces strong specific T-cell responses that remain detectable for at least two years in animal blood (25). Here, we characterized the innate responses induced locally following vaccination with the auxoGTUmultiSIV vaccine delivered with EP (DNA/EP) and at a PBS/EP site as control in order to understand the mechanisms involved in the subsequent T cell responses.

We first characterized the local inflammation by flow cytometry and showed an early influx of $CD66^+$ granulocytes and $HALDR^+CD14^+$ monocytes/macrophages at d1 and d3 in the epidermis and in the dermis at both the PBS/EP and DNA/EP sites. A deeper phenotypic analysis of the $HLADR^+CD14^+$ subset showed that this population is heterogeneous after vaccination. Indeed, two additional populations of $HLADR^+CD14^+$ cells, absent at baseline, appeared after PBS/EP and DNA/EP: the $CD163^{mid}CD11b^{high}$ and $CD163^-CD11b^+$ cells. These two subsets are distinct from the $CD163^{high}CD11b^+$ resident dermal macrophages whose frequency remain stable following PBS/EP and DNA/EP. The $CD11b^{high}CD163^+$ subset resembles to pro-inflammatory M1 macrophages, based on their lack for the CD206, a marker associated with tissue and M2 macrophages, and their recruitment under inflammatory conditions (59, 60, 63). However, they also express some markers usually associated with M2 macrophages such as a high level of CD11b and a lower level of CD40 and CD86 compared with resident macrophages. These results confirmed the high plasticity of macrophages (60, 63–65), in which macrophages share markers associated with the M1 or M2 type, depending on the inflammatory condition. The $CD163^-$ cells may correspond to blood monocytes recently recruited in the skin following injection and EP (66, 67). These $CD163^-$ cells could be in a

process of differentiation into inflammatory macrophages ($CD163^{+}CD11b^{high}$) or inflammatory DC or may serve as blood precursors to repopulate the skin of resident populations as demonstrated in different studies (44, 68, 69). Nevertheless, further investigations are required to confirm the accurate contribution of these monocytes/macrophages during the early phase of the auxoGTU with EP vaccination strategy and determine the ontological relationship between these populations.

In parallel, we observed in the epidermis the influx of an additional population of CD1a-expressing cells, distinct from $CD1a^{high}HLADR^{high}$ LCs. These cells expressed CD1a at a lower level than LCs and, in contrast to LCs, expressed CD1c and do not express CD207 at their surface. They may correspond to inflammatory dendritic epidermal cells (IDEC), which were described in the human epidermis (70, 71) and dermis (72, 73) upon inflammation. However, a proportion of these $CD1a^{int}$ cells expressed CD207 in the intracellular compartment, indicating that they may also be related to LCs. Indeed, their recruitment in an inflammatory context suggests that they might even be LC precursors as described in several mouse studies (74, 75). In addition, these $CD1a^{int}$ $CD1c^{+}$ cells increased CD1a and decreased CD1c expression over time after vaccination to acquire a phenotype closer to LCs, strengthening the hypothesis that these cells are LC precursors.

We previously showed that EP influences the intensity and localization of Ag expression in the skin (25). Without EP, Ag expression was exclusively produced in the dermis, while with EP, Ag expression was still found in the dermis but also in large amounts in the epidermis, especially in the superior differentiated keratinocyte layers (52). At baseline, LCs are localized close to the basement membrane. Previously, we have shown by *in vivo* fiber confocal

591 microscopy (76) that DNA vaccination with EP increased LC mobility and induced their
592 migration through the superior epidermal layer, where Ag was produced in the highest amounts,
593 while immunization without EP did not affect LCs localization or density (25). Here, we
594 confirmed the effect of EP on LC mobility through a transient increase of LCs in the epidermis
595 at d1 at DNA/EP and PBS/EP sites. This increase was associated with the up-regulation of
596 CD86, CD83, and HLA–DR, illustrating LC maturation, and followed by a decrease in LC
597 frequency by d3, suggesting a migration of LCs to the skin-draining lymph nodes (77).

598

599 Otherwise, this study highlighted that similar events occurred at the PBS/EP and DNA/EP
600 injection sites. These observations strongly suggest that EP was the main inducer of these
601 events, with only a marginal contribution of the auxoGTU DNA vaccine. Initially, EP was used
602 to enhance DNA entrance into cells to increase Ag production and improve subsequent specific
603 immune responses (78–80). However, our data, together with the results of other groups (78,
604 80–83), suggest that the role of EP is not limited to an increase of Ag synthesis. Actually, EP
605 causes low-intensity tissue damage which rapidly resolves, leading to inflammatory response.
606 This inflammatory response was suspected to be essential for the activation of the immune
607 system and enhancement of the adaptive response, and that, independently of the Ag quantity
608 increase due to EP (80, 81). Peng *et al.* demonstrated in a mouse Hepatitis B virus DNA vaccine
609 model that EP applied before the DNA vaccine injection resulted in an enhanced antibody
610 response similar to, or even stronger, than the response obtained when EP was applied just after
611 DNA administration (80). Additionally, our transcriptomic data showed that several genes
612 involved in skin-cell proliferation and tissue repair were differentially expressed after both
613 PBS/EP and DNA/EP. FOXM1 for example, is a transcription factor known to play a key role
614 in cell-cycle progression. This protein is required for the proper execution of mitosis and has
615 an important role in tissue repair after injury in adults (84, 85). We also observed an up-

616 regulation of *TP63* and *SPDEF*. TP63 has a crucial role in skin development and maintenance
617 (86) and is strongly up-regulated in hyperproliferative epidermal cells during normal skin
618 wound healing in mice. SPDEF is mainly associated with cancer, but Yang *et al.* reported a
619 significant up-regulation of *SPDEF* in expanded skin relative to normal skin in humans (87).
620 Altogether, these up-regulated genes may thus have a role in skin repair, notably by inducing
621 cell proliferation in response to the low tissue damage induced by EP.

622

623 Even if the cytometry analysis did not reveal a strong difference between PBS/EP and DNA/EP,
624 a deep analysis of soluble proteins and transcripts expressions highlighted subtle modifications
625 on the innate response. Indeed confirmed at the protein level that different responses were
626 induced at the PBS/EP and DNA/EP injection sites. The DNA vaccine specifically stimulated
627 skin cells by enhancing their ability to release soluble factors. MCP-1, IL-15, IL-18, and
628 sCD40-L were produced in significantly higher amounts in at least one skin compartment, and
629 mostly in the dermis. A trend of increased production of IL-8, MIP-1β, IL-10, IL-1RA, and
630 TNF-α also occurred in the presence of the DNA vaccine. Chemokines and cytokines are
631 essential for inducing cell recruitment, their activation, as well as the orientation of the immune
632 response (88). Notably, DC maturation is crucial for T-cell activation. In the absence of proper
633 inflammatory signals, DCs can migrate and present Ag to T cells, without being fully mature.
634 Under these conditions, DCs can induce T-cell anergy or direct differentiation to tolerogenic T
635 cells (89, 90). IL-15 is crucial for $CD8^+$ T-cells activation (91–93). Here, we found that IL-15
636 was produced only in the presence of the auxoGTU DNA vaccine. We hypothesize that the
637 activation of LCs by EP, in combination with enhanced IL-15 release due to the auxoGTU
638 vaccine, may be crucial for the strong activation of $CD8^+$ T cells. Overall, these results suggest
639 that EP and the auxoGTU DNA vaccine differentially stimulate skin cells and act in concert to
640 activate innate immunity (78).

641 The analysis of the transcription profile confirmed our multiplex results. Indeed, several genes
642 encoding chemokines, such as *CXCL10*, *CXCL11*, *CCL5*, and *IL8*, were induced with a stronger
643 intensity at the DNA/EP site. Additionally, we show at the transcriptomic level that a large
644 number of genes involved in immune responses, (*CCL3*, *SAA-4*, or *SIRT-6)*, and different
645 interferon-inducible genes (*STAT2*, *MX1*, *IFIH1*, *OAS2)*, that play a crucial role in antiviral
646 responses, were significantly up-regulated in the presence of the auxoGTU DNA vaccine.

647

648 The auxoGTU vectors are expressed in the *E. coli* expression system and therefore contain CpG
649 motifs. DNA vaccines mimic viral infection and our results demonstrate that this vaccination
650 strategy induces a specific transcriptional antiviral signature, probably in response to PRR
651 stimulation by the auxoGTUmultiSIV vaccine, leading to interferon production. However, the
652 characterization of the PRRs involved in this DNA vaccine recognition needs to be further
653 investigated. Our microarray data suggest a TLR involvement, as we observed a stronger
654 upregulation of MyD88 at the DNA/EP than at the PBS/EP site at d1. However, there was no
655 change in *TLR9* expression, which plays a role in the recognition of unmethylated CpG motifs
656 contained in bacterial plasmids, suggesting that this TLR is not involved in this vaccination
657 strategy. Although several studies have shown that TLR9 was required for DNA vaccine
658 efficacy (94, 95), others have demonstrated that TLR9 was dispensable for DNA vaccine
659 recognition (96–98) and specific immune response induction, suggesting other receptors
660 involvement in DNA vaccine sensing. We also observed an up-regulation of *TLR3* at d1 post-
661 vaccination, albeit only in presence of DNA. TLR3 is a dsRNA sensor localized in the
662 endosome. RNA polymerase III has also been reported to recognize foreign dsDNA and convert
663 it into dsRNA, which can trigger RIG-I, located in the cytoplasm (99). Our transcriptomic data
664 showed an up-regulation of the gene *POL3RK* encoding for the RNA polymerase III both at the
665 PBS/EP and DNA/EP sites. We can hypothesis that the auxoGTU DNA vaccine was recognized

and converted into dsRNA by the RNA polymerase III, which can trigger dsRNA sensors, such as TLR3. These results together with the specific antiviral transcriptome signature might suggest an indirect adjuvant effect of the auxoGTU DNA vaccine through the stimulation of the TLR3 axis.

Interestingly, in this study, among cytosolic DNA sensors, *AIM-2* was the only gene strongly up-regulated at d1 in the presence of DNA. This gene encodes a PRR directly involved in dsDNA recognition. After binding to dsDNA, AIM-2 shapes one form of the inflammasome, leading to the cleavage of pro-interleukin 1β and 18 to their active forms by caspase 1. Interestingly, our results showed an up-regulation of *CASP1*, the gene coding the caspase1 but only in the presence of the auxo-GTU vaccine. AIM-2 is an important DNA sensor involved in the efficacy of DNA vaccination strategies and its depletion dramatically decreased humoral and cellular antigen-specific responses in an influenza DNA vaccination mouse model (61). It was also recently demonstrated that stimulating the AIM-2 axis enhances long-lasting specific $CD8^+$ T-cell responses (100). Here, we also observed trends of positive correlations between the transcription of AIM-2 and several interferon inducible genes such as *IFIT3*, *MX1*, *MX2*, *HERC5* or *OAS2*. These data tend to confirm in a non-human primate model the involvement of AIM-2 in the sensing of DNA vaccine and the activation of the immune system, by enhancing the antiviral responses axis through interferon inducible genes.

In conclusion, we demonstrated that this vaccination strategy allowed an efficient stimulation of innate immunity, in which EP and the auxoGTU DNA vaccine differentially stimulated local cells, leading to a combined activation of innate immunity. EP acted as a strong adjuvant able to induce inflammatory-cell recruitment and LC mobilization, whereas the auxoGTUmultiSIV

690 vaccine seemed to be required to provide a specific signal to skin cells, probably through
691 various PRRs, (potential direct involvement of AIM-2 and indirectly involvement of TLR3)
692 leading to the release of soluble factors, such as IL-15, and the activation of antiviral immunity
693 through the up-regulation of several interferon-inducible genes. Altogether, these events may
694 be required for a proper DC activation, resulting in the strong stimulation of the adaptive
695 cellular immunity.

696

Acknowledgments

This work benefited from the technical support of the ASW, L2I, and LFC groups of the IDMIT infrastructure. We would like to thank Susann Fält and David Brodin at the BEA core facility at Karolinska Institutet for technical support.

Author contributions

Conceptualization: LA, RLG, MU, and FM. Methodology: LA, BT, CC, RLG, and FM. Validation: LA, BT, CJ, CP, CC, MU, ALS, and FM. Formal Analysis: LA and NT. Investigation: LA, NT, RLG, and FM; Writing of the Original Draft: LA, NT, FM; Review & Editing of the Manuscript: LA, NT, BT, PR, CJ, CP, CC, ALS, MU, RLG, and FM. Funding Acquisition: CC, MU, RLG, and FM. Supervision: RLG, and FM.

References

1. Plotkin, S. 2014. History of vaccination. *Proc. Natl. Acad. Sci.* .

2. Humphreys, I. R., and S. Sebastian. 2018. Novel viral vectors in infectious diseases. *Immunology* .

3. Santoro Rosa, D., J. de S. Apostólico, and S. B. Boscardin. 2015. DNA Vaccines: How Much Have We Accomplished In The Last 25 Years? *J. Vaccines Vaccin.* 06.

4. Cardoso, a I., M. Blixenkrone-Moller, J. Fayolle, M. Liu, R. Buckland, and T. F. Wild. 1996. Immunization with plasmid DNA encoding for the measles virus hemagglutinin and nucleoprotein leads to humoral and cell-mediated immunity. *Virology* 225: 293–9.

5. Tang, D. C., M. DeVit, and S. A. Johnston. 1992. Genetic immunization is a simple method for eliciting an immune response. *Nature* 356: 152–4.

6. Ulmer, J. B., J. J. Donnelly, S. E. Parker, G. H. Rhodes, P. L. Felgner, V. J. Dwarki, S. H. Gromkowski, R. R. Deck, C. M. DeWitt, and a Friedman. 1993. Heterologous protection against influenza by injection of DNA encoding a viral protein. *Science* 259: 1745–9.

7. Shedlock, D. J., and D. B. Weiner. 2000. DNA vaccination: antigen presentation and the induction of immunity. *J. Leukoc. Biol.* 68: 793–806.

8. Schmaljohn, C. S., K. W. Spik, and J. W. Hooper. 2014. DNA vaccines for HFRS: Laboratory and clinical studies. *Virus Res.* 187: 91–96.

9. Grant-Klein, R. J., N. M. Van Deusen, C. V. Badger, D. Hannaman, L. C. Dupuy, and C. S. Schmaljohn. 2012. A multiagent filovirus DNA vaccine delivered by intramuscular electroporation completely protects mice from ebola and Marburg virus challenge. *Hum. Vaccin. Immunother.* 8: 1703–1706.

10. Grant-Klein, R. J., L. A. Altamura, C. V Badger, C. E. Bounds, N. M. Van Deusen, S. A. Kwilas, H. A. Vu, K. L. Warfield, J. W. Hooper, D. Hannaman, L. C. Dupuy, and C. S. Schmaljohn. 2015. Codon-optimized filovirus DNA vaccines delivered by intramuscular electroporation protect cynomolgus macaques from lethal Ebola and Marburg virus challenges. *Hum. Vaccin. Immunother.* 11: 1991–2004.

11. Casimiro, D. R., L. Chen, T.-M. Fu, R. K. Evans, M. J. Caulfield, M.-E. Davies, A. Tang, M. Chen, L. Huang, V. Harris, D. C. Freed, K. A. Wilson, S. Dubey, D.-M. Zhu, D. Nawrocki, H. Mach, R. Troutman, L. Isopi, D. Williams, W. Hurni, Z. Xu, J. G. Smith, S. Wang, X. Liu, L. Guan, R. Long, W. Trigona, G. J. Heidecker, H. C. Perry, N. Persaud, T. J. Toner, Q. Su, X. Liang, R. Youil, M. Chastain, A. J. Bett, D. B. Volkin, E. A. Emini, and J. W. Shiver. 2003. Comparative immunogenicity in rhesus monkeys of DNA plasmid, recombinant vaccinia virus, and replication-defective adenovirus vectors expressing a human immunodeficiency virus type 1 gag gene. *J. Virol.* 77: 6305–13.

12. Fynan, E. F., R. G. Webster, D. H. Fuller, J. R. Haynes, J. C. Santoro, and H. L. Robinson. 1993. DNA vaccines: protective immunizations by parenteral, mucosal, and gene-gun inoculations. *Proc. Natl. Acad. Sci. U. S. A.* 90: 11478–82.

13. Hannaman, D., L. C. Dupuy, B. Ellefsen, and C. S. Schmaljohn. 2016. A Phase 1 clinical trial of a DNA vaccine for Venezuelan equine encephalitis delivered by intramuscular or intradermal electroporation. *Vaccine* 34: 3607–3612.

14. Hooper, J. W., J. E. Moon, K. M. Paolino, R. Newcomer, D. E. McLain, M. Josleyn, D. Hannaman, and C. Schmaljohn. 2014. A Phase 1 clinical trial of Hantaan virus and Puumala virus M-segment DNA vaccines for haemorrhagic fever with renal syndrome delivered by intramuscular electroporation. *Clin. Microbiol. Infect.* 20: 110–117.

15. Vardas, E., I. Stanescu, M. Leinonen, K. Ellefsen, G. Pantaleo, M. Valtavaara, M. Ustav, and K. Reijonen. 2012. Indicators of therapeutic effect in FIT-06, a Phase II trial of a DNA vaccine, GTU(®)-Multi-HIVB, in untreated HIV-1 infected subjects. *Vaccine* 30: 4046–54.

16. Wang, S., D. J. Farfan-Arribas, S. Shen, T.-H. W. Chou, A. Hirsch, F. He, and S. Lu. 2006. Relative contributions of codon usage, promoter efficiency and leader sequence to the antigen expression and immunogenicity of HIV-1 Env DNA vaccine. *Vaccine* 24: 4531–40.

17. Ulmer, J. B., B. Wahren, and M. a Liu. 2006. Gene-based vaccines: recent technical and clinical advances. *Trends Mol. Med.* 12: 216–22.

18. Liu, M. a, B. Wahren, and G. B. Karlsson Hedestam. 2006. DNA vaccines: recent developments and future possibilities. *Hum. Gene Ther.* 17: 1051–61.

19. Krohn, K., I. Stanescu, V. Blazevic, T. Vesikari, A. Ranki, and M. Ustav. 2005. A DNA HIV-1 vaccine based on a fusion gene expressing non-structural and structural genes of consensus sequence of the A-C subtypes and the ancestor sequence of the F-H subtypes. Preclinical and clinical studies. *Microbes Infect.* 7: 1405–13.

20. Djuranovic, D., C. Oguey, and B. Hartmann. 2004. The role of DNA structure and dynamics in the recognition of bovine papillomavirus E2 protein target sequences. *J. Mol. Biol.* 339: 785–96.

21. Blazevic, V., A. Männik, M. Malm, R. Sikut, M. Valtavaara, U. Toots, M. Ustav, and K. Krohn. 2006. Induction of human immunodeficiency virus type-1-specific immunity with a novel gene transport unit (GTU)-MultiHIV DNA vaccine. *AIDS Res. Hum. Retroviruses* 22: 667–77.

22. Wang, Z., P. J. Troilo, X. Wang, T. G. Griffiths, S. J. Pacchione, a B. Barnum, L. B. Harper, C. J. Pauley, Z. Niu, L. Denisova, T. T. Follmer, G. Rizzuto, G. Ciliberto, E. Fattori, N. L. Monica, S. Manam, and B. J. Ledwith. 2004. Detection of integration of plasmid DNA into host genomic DNA following intramuscular injection and electroporation. *Gene Ther.* 11: 711–21.

23. Hutnick, N. a, D. J. F. Myles, C. B. Bian, K. Muthumani, and D. B. Weiner. 2011. Selected approaches for increasing HIV DNA vaccine immunogenicity in vivo. *Curr. Opin. Virol.* 1: 233–40.

24. Hirao, L. a, L. Wu, A. Satishchandran, A. S. Khan, R. Draghia-Akli, A. C. Finnefrock, A. J. Bett, M. R. Betts, D. R. Casimiro, N. Y. Sardesai, J. J. Kim, J. W. Shiver, and D. B. Weiner. 2010. Comparative analysis of immune responses induced by vaccination with SIV antigens by recombinant Ad5 vector or plasmid DNA in rhesus macaques. *Mol. Ther.* 18: 1568–76.

25. Martinon, F., K. Kaldma, R. Sikut, S. Culina, G. Romain, M. Tuomela, M. Adojaan, A. Männik, U. Toots, T. Kivisild, J. Morin, P. Brochard, B. Delache, A. Tripiciano, F. Ensoli, I. Stanescu, R. Le Grand, and M. Ustav. 2009. Persistent immune responses induced by a human immunodeficiency virus DNA vaccine delivered in association with electroporation in the skin of nonhuman primates. *Hum. Gene Ther.* 20: 1291–307.

26. Rosati, M., A. Valentin, R. Jalah, V. Patel, A. von Gegerfelt, C. Bergamaschi, C. Alicea, D. Weiss, J. Treece, R. Pal, P. D. Markham, E. T. a Marques, J. T. August, A. Khan, R. Draghia-Akli, B. K. Felber, and G. N. Pavlakis. 2008. Increased immune responses in rhesus macaques by DNA vaccination combined with electroporation. *Vaccine* 26: 5223–9.

27. Trimble, C. L., M. P. Morrow, K. A. Kraynyak, X. Shen, M. Dallas, J. Yan, L. Edwards, R. L. Parker, L. Denny, M. Giffear, A. S. Brown, K. Marcozzi-Pierce, D. Shah, A. M. Slager, A. J. Sylvester, A. Khan, K. E. Broderick, R. J. Juba, T. A. Herring, J. Boyer, J. Lee, N. Y.

Sardesai, D. B. Weiner, and M. L. Bagarazzi. 2015. Safety, efficacy, and immunogenicity of VGX-3100, a therapeutic synthetic DNA vaccine targeting human papillomavirus 16 and 18 E6 and E7 proteins for cervical intraepithelial neoplasia 2/3: A randomised, double-blind, placebo-controlled phase 2b trial. *Lancet* 386: 2078–2088.

28. Kim, T. J., H. T. Jin, S. Y. Hur, H. G. Yang, Y. B. Seo, S. R. Hong, C. W. Lee, S. Kim, J. W. Woo, K. S. Park, Y. Y. Hwang, J. Park, I. H. Lee, K. T. Lim, K. H. Lee, M. S. Jeong, C. D. Surh, Y. S. Suh, J. S. Park, and Y. C. Sung. 2014. Clearance of persistent HPV infection and cervical lesion by therapeutic DNA vaccine in CIN3 patients. *Nat. Commun.* 5.

29. Combadiere, B., and C. Liard. 2011. Transcutaneous and intradermal vaccination. *Hum. Vaccin.* 7: 811–827.

30. Gonçalves, E., O. Bonduelle, A. Soria, P. Loulergue, A. Rousseau, M. Cachanado, H. Bonnabau, R. Thiebaut, N. Tchitchek, S. Behillil, S. van der Werf, A. Vogt, T. Simon, O. Launay, and B. Combadière. 2019. Innate gene signature distinguishes humoral versus cytotoxic responses to influenza vaccination. *J. Clin. Invest.* 129: 1960–1971.

31. Klechevsky, E. 2013. Human dendritic cells - stars in the skin. *Eur. J. Immunol.* 43: 3147–3155.

32. Kim, Y. C., C. Jarrahian, D. Zehrung, S. Mitragotri, and M. R. Prausnitz. 2012. Delivery systems for intradermal vaccination. *Curr. Top. Microbiol. Immunol.* 351: 77–112.

33. Fernando, G. J. P., X. Chen, T. W. Prow, M. L. Crichton, E. J. Fairmaid, M. S. Roberts, I. H. Frazer, L. E. Brown, and M. A. F. Kendall. 2010. Potent Immunity to Low Doses of Influenza Vaccine by Probabilistic Guided Micro-Targeted Skin Delivery in a Mouse Model. *PLoS One* 5: e10266.

34. Adam, L., P. Rosenbaum, A. Cosma, R. Le Grand, and F. Martinon. 2015. Identification of skin immune cells in non-human primates. *J. Immunol. Methods* 426: 42–49.

35. Romain, G., E. Van Gulck, O. Epaulard, S. Oh, D. Li, G. Zurawski, S. Zurawski, A. Cosma, L. Adam, C. Chapon, B. Todorova, J. Banchereau, N. Dereuddre-Bosquet, G. Vanham, R. Le Grand, and F. Martinon. 2012. CD34-derived dendritic cells transfected ex vivo with HIV-Gag mRNA induce polyfunctional T-cell responses in nonhuman primates. *Eur. J. Immunol.* 42: 2019–2033.

36. Epaulard, O., L. Adam, C. Poux, G. Zurawski, N. Salabert, P. Rosenbaum, N. Dereuddre-Bosquet, S. Zurawski, A.-L. Flamar, S. Oh, G. Romain, C. Chapon, J. Banchereau, Y. Lévy, R. Le Grand, and F. Martinon. 2014. Macrophage- and neutrophil-derived TNF-α instructs skin langerhans cells to prime antiviral immune responses. *J. Immunol.* 193: 2416–26.

37. Ouchi, T., A. Kubo, M. Yokouchi, T. Adachi, T. Kobayashi, D. Y. Kitashima, H. Fujii, B. E. Clausen, S. Koyasu, M. Amagai, and K. Nagao. 2011. Langerhans cell antigen capture through tight junctions confers preemptive immunity in experimental staphylococcal scalded skin syndrome. *J. Exp. Med.* 208: 2607–13.

38. Gao, Y., S. a Nish, R. Jiang, L. Hou, P. Licona-Limón, J. S. Weinstein, H. Zhao, and R. Medzhitov. 2013. Control of T helper 2 responses by transcription factor IRF4-dependent dendritic cells. *Immunity* 39: 722–32.

39. Haniffa, M., A. Shin, V. Bigley, N. McGovern, P. Teo, P. See, P. S. Wasan, X.-N. Wang, F. Malinarich, B. Malleret, A. Larbi, P. Tan, H. Zhao, M. Poidinger, S. Pagan, S. Cookson, R. Dickinson, I. Dimmick, R. F. Jarrett, L. Renia, J. Tam, C. Song, J. Connolly, J. K. Y. Chan, A. Gehring, A. Bertoletti, M. Collin, and F. Ginhoux. 2012. Human tissues contain CD141hi cross-presenting dendritic cells with functional homology to mouse CD103+ nonlymphoid dendritic cells. *Immunity* 37: 60–73.

40. Klechevsky, E., R. Morita, M. Liu, Y. Cao, S. Coquery, L. A. Thompson-Snipes, F. Briere, D. Chaussabel, G. Zurawski, A. K. Palucka, Y. Reiter, J. Banchereau, and H. Ueno. 2008. Functional Specializations of Human Epidermal Langerhans Cells and CD14+Dermal Dendritic Cells. *Immunity* 29: 497–510.

41. Kumamoto, Y., M. Linehan, J. S. Weinstein, B. J. Laidlaw, J. E. Craft, and A. Iwasaki. 2013. CD301b^{+} dermal dendritic cells drive T helper 2 cell-mediated immunity. *Immunity* 39: 733–43.

42. Ochoa, M. T., A. Loncaric, S. R. Krutzik, T. C. Becker, and R. L. Modlin. 2008. "Dermal dendritic cells" comprise two distinct populations: CD1+ dendritic cells and CD209+ macrophages. *J. Invest. Dermatol.* 128: 2225–31.

43. Zaba, L. C., J. Fuentes-Duculan, R. M. Steinman, J. G. Krueger, and M. A. Lowes. 2007. Normal human dermis contains distinct populations of CD11c+BDCA-1+ dendritic cells and CD163+FXIIIA+ macrophages. *J. Clin. Invest.* 117: 2517–25.

44. Haniffa, M., F. Ginhoux, X.-N. Wang, V. Bigley, M. Abel, I. Dimmick, S. Bullock, M. Grisotto, T. Booth, P. Taub, C. Hilkens, M. Merad, and M. Collin. 2009. Differential rates of replacement of human dermal dendritic cells and macrophages during hematopoietic stem cell transplantation. *J. Exp. Med.* 206: 371–85.

45. Rodero, M. P., and K. Khosrotehrani. 2010. Skin wound healing modulation by macrophages. *Int. J. Clin. Exp. Pathol.* 3: 643–53.

46. Gordon, S., and P. R. Taylor. 2005. Monocyte and macrophage heterogeneity. *Nat. Rev. Immunol.* 5: 953–64.

47. Mosser, D. M., and J. P. Edwards. 2008. Exploring the full spectrum of macrophage activation. *Nat. Rev. Immunol.* 8: 958–69.

48. Pulendran, B., and R. Ahmed. 2011. Immunological mechanisms of vaccination. *Nat. Immunol.* 12: 509–517.

49. Seneschal, J., R. a Clark, A. Gehad, C. M. Baecher-Allan, and T. S. Kupper. 2012. Human epidermal Langerhans cells maintain immune homeostasis in skin by activating skin resident regulatory T cells. *Immunity* 36: 873–84.

50. Duffy, D., H. Perrin, V. Abadie, N. Benhabiles, A. Boissonnas, C. Liard, B. Descours, D. Reboulleau, O. Bonduelle, B. Verrier, N. Van Rooijen, C. Combadière, and B. Combadière. 2012. Neutrophils transport antigen from the dermis to the bone marrow, initiating a source of memory CD8+ T cells. *Immunity* 37: 917–29.

51. Querec, T., S. Bennouna, S. Alkan, Y. Laouar, K. Gorden, R. Flavell, S. Akira, R. Ahmed, and B. Pulendran. 2006. Yellow fever vaccine YF-17D activates multiple dendritic cell subsets via TLR2, 7, 8, and 9 to stimulate polyvalent immunity. *J. Exp. Med.* 203: 413–24.

52. Todorova, B., L. Adam, S. Culina, R. Boisgard, A. Cosma, M. Ustav, T. Kortulewski, and R. Le Grand. 2017. Electroporation as a vaccine delivery system and a natural adjuvant to intradermal administration of plasmid DNA in macaques. 1–11.

53. Adam, L., R. Le Grand, and F. Martinon. 2014. Electroporation-Mediated Intradermal Delivery of DNA Vaccines in Nonhuman Primates. In Humana Press, New York, NY. 309–313.

54. Bond, E., W. C. Adams, A. Smed-Sörensen, K. J. Sandgren, L. Perbeck, A. Hofmann, J. Andersson, and K. Loré. 2009. Techniques for time-efficient isolation of human skin dendritic cell subsets and assessment of their antigen uptake capacity. *J. Immunol. Methods* 348: 42–56.

55. Stoitzner, P., N. Romani, A. D. McLellan, C. H. Tripp, and S. Ebner. 2010. Isolation of

skin dendritic cells from mouse and man. *Methods Mol. Biol.* 595: 235–48.

56. Bécavin, C., N. Tchitchek, C. Mintsa-Eya, A. Lesne, and A. Benecke. 2011. Improving the efficiency of multidimensional scaling in the analysis of high-dimensional data using singular value decomposition. *Bioinformatics* 27: 1413–21.

57. Kruskal, J. B., and M. Wish. 1978. *Multidimensional Scaling, Numéro 11*,.

58. Zaba, L. C., J. G. Krueger, and M. a Lowes. 2009. Resident and "inflammatory" dendritic cells in human skin. *J. Invest. Dermatol.* 129: 302–8.

59. Ambarus, C. a, S. Krausz, M. van Eijk, J. Hamann, T. R. D. J. Radstake, K. a Reedquist, P. P. Tak, and D. L. P. Baeten. 2012. Systematic validation of specific phenotypic markers for in vitro polarized human macrophages. *J. Immunol. Methods* 375: 196–206.

60. Vogel, D. Y. S., E. J. F. Vereyken, J. E. Glim, P. D. a M. Heijnen, M. Moeton, P. van der Valk, S. Amor, C. E. Teunissen, J. van Horssen, and C. D. Dijkstra. 2013. Macrophages in inflammatory multiple sclerosis lesions have an intermediate activation status. *J. Neuroinflammation* 10: 35.

61. Suschak, J. J., S. Wang, K. A. Fitzgerald, and S. Lu. 2015. Identification of Aim2 as a sensor for DNA vaccines. *J. Immunol.* 194: 630–6.

62. Kasturi, S. P., I. Skountzou, R. A. Albrecht, D. Koutsonanos, T. Hua, H. I. Nakaya, R. Ravindran, S. Stewart, M. Alam, M. Kwissa, F. Villinger, N. Murthy, J. Steel, J. Jacob, R. J. Hogan, A. García-Sastre, R. Compans, and B. Pulendran. 2011. Programming the magnitude and persistence of antibody responses with innate immunity. *Nature* 470: 543–7.

63. Zeyda, M., D. Farmer, J. Todoric, O. Aszmann, M. Speiser, G. Györi, G. J. Zlabinger, and T. M. Stulnig. 2007. Human adipose tissue macrophages are of an anti-inflammatory phenotype but capable of excessive pro-inflammatory mediator production. *Int. J. Obes. (Lond).* 31: 1420–8.

64. Porcheray, F., S. Viaud, a-C. Rimaniol, C. Léone, B. Samah, N. Dereuddre-Bosquet, D. Dormont, and G. Gras. 2005. Macrophage activation switching: an asset for the resolution of inflammation. *Clin. Exp. Immunol.* 142: 481–9.

65. Fuentes-Duculan, J., M. Suárez-Fariñas, L. C. Zaba, K. E. Nograles, K. C. Pierson, H. Mitsui, C. a Pensabene, J. Kzhyshkowska, J. G. Krueger, and M. a Lowes. 2010. A subpopulation of CD163-positive macrophages is classically activated in psoriasis. *J. Invest. Dermatol.* 130: 2412–22.

66. Tamoutounour, S., M. Guilliams, F. Montanana Sanchis, H. Liu, D. Terhorst, C. Malosse, E. Pollet, L. Ardouin, H. Luche, C. Sanchez, M. Dalod, B. Malissen, and S. Henri. 2013. Origins and Functional Specialization of Macrophages and of Conventional and Monocyte-Derived Dendritic Cells in Mouse Skin. *Immunity* 39: 925–938.

67. Jakubzick, C., E. L. Gautier, S. L. Gibbings, D. K. Sojka, A. Schlitzer, T. E. Johnson, S. Ivanov, Q. Duan, S. Bala, T. Condon, N. van Rooijen, J. R. Grainger, Y. Belkaid, A. Ma'ayan, D. W. H. Riches, W. M. Yokoyama, F. Ginhoux, P. M. Henson, and G. J. Randolph. 2013. Minimal differentiation of classical monocytes as they survey steady-state tissues and transport antigen to lymph nodes. *Immunity* 39: 599–610.

68. Greter, M., I. Lelios, P. Pelczar, G. Hoeffel, J. Price, M. Leboeuf, T. M. Kündig, K. Frei, F. Ginhoux, M. Merad, and B. Becher. 2012. Stroma-derived interleukin-34 controls the development and maintenance of langerhans cells and the maintenance of microglia. *Immunity* 37: 1050–60.

69. Yona, S., K.-W. Kim, Y. Wolf, A. Mildner, D. Varol, M. Breker, D. Strauss-Ayali, S.

936 Viukov, M. Guilliams, A. Misharin, D. a Hume, H. Perlman, B. Malissen, E. Zelzer, and S.
937 Jung. 2013. Fate mapping reveals origins and dynamics of monocytes and tissue macrophages
938 under homeostasis. *Immunity* 38: 79–91.

939 70. Wollenberg, A., and M. Mommaas. 2002. Expression and function of the mannose
940 receptor CD206 on epidermal dendritic cells in inflammatory skin diseases. *J. Invest.*
941 *Dermatol.* 118: 327–334.

942 71. Dijkstra, D., H. Stark, P. L. Chazot, F. C. Shenton, R. Leurs, T. Werfel, and R. Gutzmer.
943 2008. Human inflammatory dendritic epidermal cells express a functional histamine H4
944 receptor. *J. Invest. Dermatol.* 128: 1696–703.

945 72. Chu, C.-C., P. Di Meglio, and F. O. Nestle. 2011. Harnessing dendritic cells in
946 inflammatory skin diseases. *Semin. Immunol.* 23: 28–41.

947 73. Guttman-Yassky, E., M. a Lowes, J. Fuentes-Duculan, J. Whynot, I. Novitskaya, I.
948 Cardinale, A. Haider, A. Khatcherian, J. a Carucci, R. Bergman, and J. G. Krueger. 2007.
949 Major differences in inflammatory dendritic cells and their products distinguish atopic
950 dermatitis from psoriasis. *J. Allergy Clin. Immunol.* 119: 1210–7.

951 74. Seré, K., J.-H. Baek, J. Ober-Blöbaum, G. Müller-Newen, F. Tacke, Y. Yokota, M. Zenke,
952 and T. Hieronymus. 2012. Two Distinct Types of Langerhans Cells Populate the Skin during
953 Steady State and Inflammation. *Immunity* 37: 905–916.

954 75. Merad, M., M. G. Manz, H. Karsunky, A. Wagers, W. Peters, I. Charo, I. L. Weissman, J.
955 G. Cyster, and E. G. Engleman. 2002. Langerhans cells renew in the skin throughout life
956 under steady-state conditions. *Nat. Immunol.* 3: 1135–41.

957 76. Todorova, B., N. Salabert, S. Tricot, R. Boisgard, M. Rathaux, R. Le Grand, and C.
958 Chapon. 2017. Fibered Confocal Fluorescence Microscopy for the Noninvasive Imaging of
959 Langerhans Cells in Macaques. *Contrast Media Mol. Imaging* 2017: 1–8.

960 77. Moll, H., H. Fuchs, C. Blank, and M. Röllinghoff. 1993. Langerhans cells transport
961 Leishmania major from the infected skin to the draining lymph node for presentation to
962 antigen-specific T cells. *Eur. J. Immunol.* 23: 1595–601.

963 78. Roos, A.-K., F. Eriksson, J. a Timmons, J. Gerhardt, U. Nyman, L. Gudmundsdotter, A.
964 Bråve, B. Wahren, and P. Pisa. 2009. Skin electroporation: effects on transgene expression,
965 DNA persistence and local tissue environment. *PLoS One* 4: e7226.

966 79. Zhang, L., E. Nolan, S. Kreitschitz, and D. P. Rabussay. 2002. Enhanced delivery of
967 naked DNA to the skin by non-invasive in vivo electroporation. *Biochim. Biophys. Acta* 1572:
968 1–9.

969 80. Peng, B., Y. Zhao, L. Xu, and Y. Xu. 2007. Electric pulses applied prior to intramuscular
970 DNA vaccination greatly improve the vaccine immunogenicity. *Vaccine* 25: 2064–73.

971 81. Babiuk, S., M. E. Baca-Estrada, M. Foldvari, D. M. Middleton, D. Rabussay, G. Widera,
972 and L. a Babiuk. 2004. Increased gene expression and inflammatory cell infiltration caused by
973 electroporation are both important for improving the efficacy of DNA vaccines. *J. Biotechnol.*
974 110: 1–10.

975 82. Liu, J., R. Kjeken, I. Mathiesen, and D. H. Barouch. 2008. Recruitment of antigen-
976 presenting cells to the site of inoculation and augmentation of human immunodeficiency virus
977 type 1 DNA vaccine immunogenicity by in vivo electroporation. *J. Virol.* 82: 5643–9.

978 83. Rizzuto, G., M. Cappelletti, D. Maione, R. Savino, D. Lazzaro, P. Costa, I. Mathiesen, R.
979 Cortese, G. Ciliberto, R. Laufer, N. La Monica, and E. Fattori. 1999. Efficient and regulated
980 erythropoietin production by naked DNA injection and muscle electroporation. *Proc. Natl.*

981 *Acad. Sci. U. S. A.* 96: 6417–22.

982 84. Wierstra, I. 2013. The transcription factor FOXM1 (Forkhead box M1): proliferation-
983 specific expression, transcription factor function, target genes, mouse models, and normal
984 biological roles. *Adv. Cancer Res.* 118: 97–398.

985 85. Wierstra, I., and J. Alves. 2007. FOXM1, a typical proliferation-associated transcription
986 factor. *Biol. Chem.* 388: 1257–74.

987 86. Koster, M. I. 2010. p63 in skin development and ectodermal dysplasias. *J. Invest.*
988 *Dermatol.* 130: 2352–8.

989 87. Yang, M., Y. Liang, L. Sheng, G. Shen, K. Liu, B. Gu, F. Meng, and Q. Li. 2011. A
990 preliminary study of differentially expressed genes in expanded skin and normal skin:
991 implications for adult skin regeneration. *Arch. Dermatol. Res.* 303: 125–33.

992 88. Kapsenberg, M. L. 2003. Dendritic-cell control of pathogen-driven T-cell polarization.
993 *Nat. Rev. Immunol.* 3: 984–93.

994 89. Hawiger, D., K. Inaba, Y. Dorsett, M. Guo, K. Mahnke, M. Rivera, J. V Ravetch, R. M.
995 Steinman, and M. C. Nussenzweig. 2001. Dendritic cells induce peripheral T cell
996 unresponsiveness under steady state conditions in vivo. *J. Exp. Med.* 194: 769–79.

997 90. Jonuleit, H., E. Schmitt, G. Schuler, J. Knop, and a H. Enk. 2000. Induction of interleukin
998 10-producing, nonproliferating CD4(+) T cells with regulatory properties by repetitive
999 stimulation with allogeneic immature human dendritic cells. *J. Exp. Med.* 192: 1213–22.

1000 91. Banchereau, J., L. Thompson-Snipes, S. Zurawski, J.-P. Blanck, Y. Cao, S. Clayton, J.-P.
1001 Gorvel, G. Zurawski, and E. Klechevsky. 2012. The differential production of cytokines by
1002 human Langerhans cells and dermal CD14(+) DCs controls CTL priming. *Blood* 119: 5742–9.

1003 92. Klebanoff, C. a, S. E. Finkelstein, D. R. Surman, M. K. Lichtman, L. Gattinoni, M. R.
1004 Theoret, N. Grewal, P. J. Spiess, P. a Antony, D. C. Palmer, Y. Tagaya, S. a Rosenberg, T. a
1005 Waldmann, and N. P. Restifo. 2004. IL-15 enhances the in vivo antitumor activity of tumor-
1006 reactive CD8+ T cells. *Proc. Natl. Acad. Sci. U. S. A.* 101: 1969–74.

1007 93. Dubsky, P., H. Saito, M. Leogier, C. Dantin, J. E. Connolly, J. Banchereau, and a K.
1008 Palucka. 2007. IL-15-induced human DC efficiently prime melanoma-specific naive CD8+ T
1009 cells to differentiate into CTL. *Eur. J. Immunol.* 37: 1678–90.

1010 94. Liu, M. a. 2010. Immunologic basis of vaccine vectors. *Immunity* 33: 504–15.

1011 95. Tudor, D., C. Dubuquoy, V. Gaboriau, F. Lefèvre, B. Charley, and S. Riffault. 2005.
1012 TLR9 pathway is involved in adjuvant effects of plasmid DNA-based vaccines. *Vaccine* 23:
1013 1258–64.

1014 96. Babiuk, S., N. Mookherjee, R. Pontarollo, P. Griebel, S. van Drunen Littel-van den Hurk,
1015 R. Hecker, and L. Babiuk. 2004. TLR9-/- and TLR9+/+ mice display similar immune
1016 responses to a DNA vaccine. *Immunology* 113: 114–20.

1017 97. Spies, B., H. Hochrein, M. Vabulas, K. Huster, D. H. Busch, F. Schmitz, A. Heit, and H.
1018 Wagner. 2003. Vaccination with plasmid DNA activates dendritic cells via Toll-like receptor
1019 9 (TLR9) but functions in TLR9-deficient mice. *J. Immunol.* 171: 5908–12.

1020 98. Ligtenberg, M. A., N. Rojas-Colonelli, R. Kiessling, and A. Lladser. 2013. NF-κB
1021 activation during intradermal DNA vaccination is essential for eliciting tumor protective
1022 antigen-specific CTL responses. *Hum. Vaccin. Immunother.* 9: 2189–95.

1023 99. Chiu, Y.-H., J. B. Macmillan, and Z. J. Chen. 2009. RNA polymerase III detects cytosolic
1024 DNA and induces type I interferons through the RIG-I pathway. *Cell* 138: 576–91.

100. Yin, L., D. Chai, Y. Yue, C. Dong, and S. Xiong. 2017. AIM2 Co-immunization with VP1 Is Associated with Increased Memory CD8 T Cells and Mounts Long Lasting Protection against Coxsackievirus B3 Challenge. *Front. Cell. Infect. Microbiol.* 7: 247.

Figure legends

Figure 1. **Vaccine-induced immune responses in non-human primates.** Animals were vaccinated at weeks 0, 4, and 12 with the auxoGTUmultiSIV vaccine, with or without EP. T-cell responses against Nef, Gag, Tat, and Rev epitopes, as well as the cumulative response against all were measured by interferon (IFN)-γ enzyme-linked immunospot (ELISpot) assays. The error bars correspond to the SEM for each group of eight or six animals on the indicated day of the experiment. Day 0 is the day of the first injection.

Figure 2. Immune cells recruited to the epidermis and dermis after injection and EP.

The percentages of immune cells are depicted over time in total epidermis cells (**A**) and dermis cells (**B**) at PBS/EP and DNA/EP injection sites. The Friedman test was used with Dunn's post-test for comparisons relative to baseline. *p < 0.05; *p < 0.01; ***p < 0.001. Comparisons between the two sites were performed using the Wilcoxon test (n = 9, three independent experiments) indicated with the bold line $^{\#}p<0.05$.

Figure 3. Three HLA–DR^{+}CD14^{+} subsets appear after injection and EP in the dermis. (A) Flow cytometry analysis of the surface expressions of CD11b and CD163 in the HLA–DR^{+}CD14^{+} population at the untreated site (baseline) and d1, d3, and d8 after DNA/EP vaccination in the epidermis and dermis of one representative animal. **(B)** Frequencies of dermal CD163^{high}CD11b^{+} (subset 1), CD163^{mid}CD11b^{high} (subset 2), and CD163^{-}CD11b^{+} (subset 3) cells measured over time at the PBS/EP and DNA/EP injection sites in the HLA–DR^{+}CD14^{+} population. The comparisons between both treatments (right panels) were performed at the peak of macrophage recruitment (d1). The Friedman test was used with Dunn's post-test for

comparisons relative to baseline. Comparisons between the two sites were performed using the Wilcoxon test (n = 8 to 9 per group, three independent experiments). *p < 0.05; **p < 0.01; ***p < 0.001. (**C**) Surface expression of different markers of the three $CD14^+$ subsets isolated at d1 after DNA/EP, showing one representative animal out of three.

Figure 4. Electroporation induces LC mobilization, their activation, and the recruitment of a $CD1a^{int}$ population distinct from LCs. (A) Flow cytometry analysis of CD1a and CD1c surface marker expressions on epidermal $CD45^+$ cells at baseline, and d1, d3, and d8 after DNA/EP vaccination for one representative animal. **(B)** Frequencies of $CD1a^+CD1c^-$ cells (subset 1) and $CD1a^{int}CD1c^+$ cells (subset 2) over time at the PBS/EP and DNA/EP injection sites. The Friedman test was used with Dunn's post-test for comparisons relative to baseline. Comparisons between the two sites were performed using the Wilcoxon test. Each line represents one animal (n = 8 or 9 per group) *p < 0.05; **p < 0.01 **(C)** Representative examples for the expressions of CD86, CD83, and HLA–DR at d1 (pink), d3 (orange), and d8 (green) relative to baseline (grey filled area) at the PBS/EP and DNA/EP injection sites. **(D)** Surface and intracellular staining of CD207 at d3 after DNA/EP of subset 1 (LC, clear red histogram) and subset 2 ($CD1a^{int}CD1c^+$ cells, clear blue histogram) with isotype controls shown in the filled histograms. The table shows the percentage of CD207-expressing cells within subset 2 ($CD1a^{int}CD1^+$ cells) for two representative animals.

Figure 5. The auxoGTUmultiSIV vaccine elicits enhanced the release of soluble factors from skin cells. Log fold-change representation of cytokines secreted in the epidermis (top panel) and dermis (bottom panel) relative to baseline at d1, d3, and d8 after PBS/EP (white, open bars) and DNA/EP (black, filled bars) treatments. ND: cytokine production under the level

of detection. Two-way ANOVA with Bonferroni post-test was used (n = 3 to 6). *p < 0.05 **p< 0.01.

Figure 6. Differential gene expression analysis of PBS/EP and DNA/EP treatments relative to the baseline. (A) Bar plot representation showing the number of up- and down-regulated genes at each time point after PBS/EP and DNA/EP relative to the baseline. Up-regulated genes are indicated by red bars and down-regulated genes by green bars. The height of the bars is proportional to the number of genes up- or down- regulated (n = 6 per group). **(B)** Multidimensional scaling (MDS) representation showing the similarities and dissimilarities between the transcriptomic profiles. Transcriptomic profiles were restricted to the list of genes found to be differentially expressed in at least one condition. Each dot in the MDS representation is a transcriptomic profile and distances between the dots are proportional to the transcriptomic distances between the biological samples. Dots are shaped to indicate the treatment and colored to indicate the time point post infection. The baseline is indicated by red-colored dots. Each biological condition is indicated by a colored convex hull. The Kruskal Stress (KS) criterion shown in the representation quantifies the quality of the representation as a fraction of the information lost during the dimensionality reduction procedure.

Figure 7. Differential gene expression analysis of PBS/EP compared to DNA/EP. (A) Heatmap showing the expression fold-change values of the differentially expressed cytokine, chemokine, chemokine receptor, and CD genes relative to baseline for at least one condition. Hierarchical clustering was performed at the gene level using the complete linkage method. The duplicate gene symbols correspond to different probes measuring the same gene. **(B)** Heatmap showing the expression fold-change values of the genes found to be differentially expressed

between the DNA/EP and PBS/EP treatments for at least one time point post-injection. Hierarchical clustering was performed at the gene level using the complete linkage method. Tree clusters of genes with similar expression patterns were found based on the hierarchical clustering.

Figure 8. TLR and cytosolic DNA sensor regulation at the transcriptome level. Gene relative expression of skin biopsy samples collected at baseline, d1, d3 and d8 at PBS/EP and DNA/EP sites for RNA encoding TLR (**A**) cytosolic DNA sensor (**B**) NOD-Like receptor *NLRP3* and *NLRP4* coding molecules and *CASP1* coding caspase1, involved in inflammasome formation **(C)** Two-way ANOVA with Bonferroni post-test was used (n = 5 to 6)*<0.05, **<0.01, ***<0.001. **(D)** The degree of correlation between the relative expression of interferon inducible genes (ISG) *MX1*, *MX2*, *IFIT3*, *HERC5*, *OAS2* and *IFNG with the* relative expression of AIM-2 at d1 at the DNA/EP site was studied

Figure 1

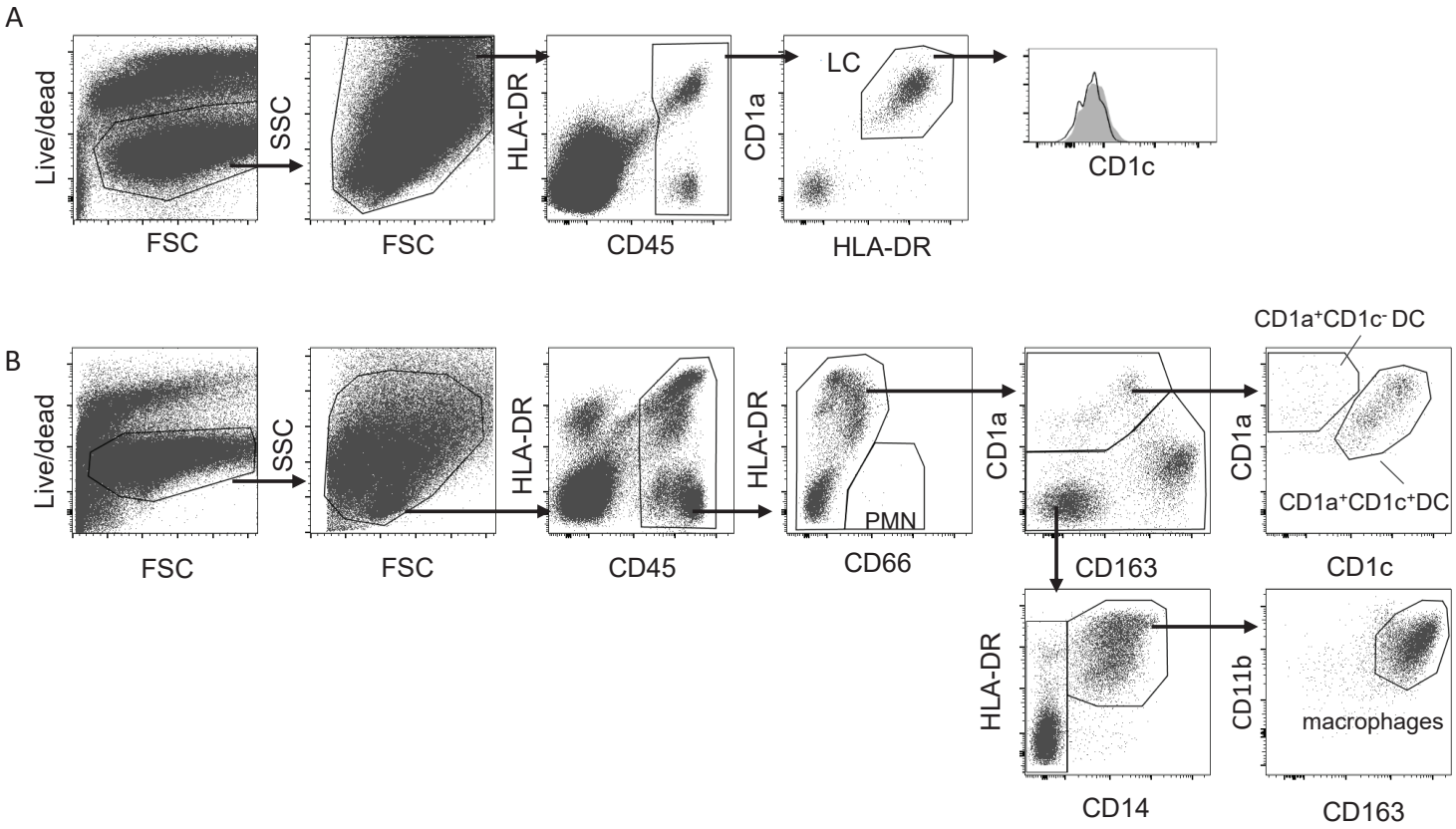
A
Live/dead
FSC
SSC
FSC
HLA-DR
CD45
CD1a
LC
HLA-DR
CD1c
B
Live/dead
FSC
SSC
FSC
HLA-DR
CD45
HLA-DR
PMN
CD66
CD1a
CD163
CD1a+CD1c- DC
CD1a
CD1a+CD1c+DC
CD1c
HLA-DR
CD14
CD11b
macrophages
CD163

Figure 2

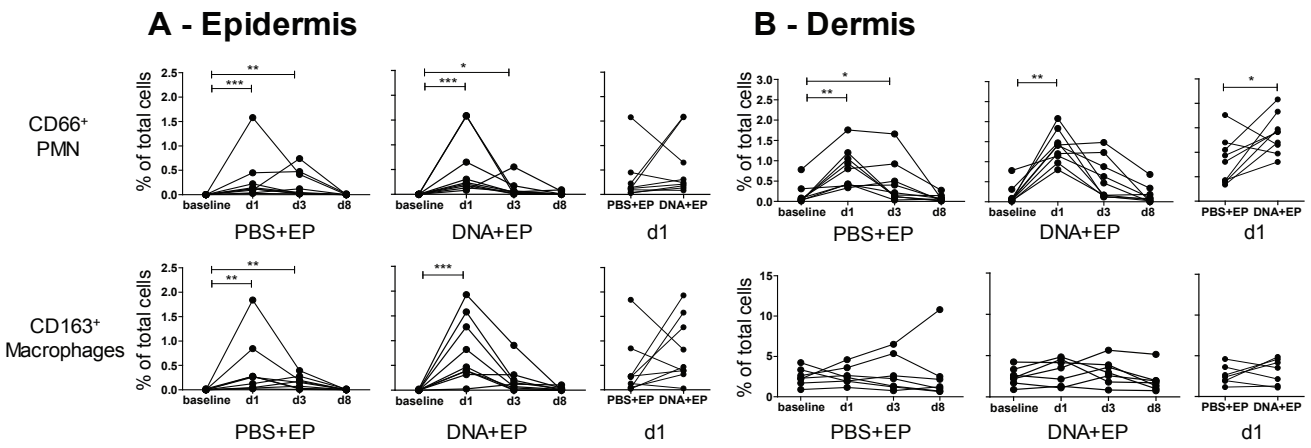
A - Epidermis
B - Dermis
CD66+ PMN
CD163+ Macrophages
% of total cells
baseline
d1
d3
d8
PBS+EP
DNA+EP
d1

Figure 3

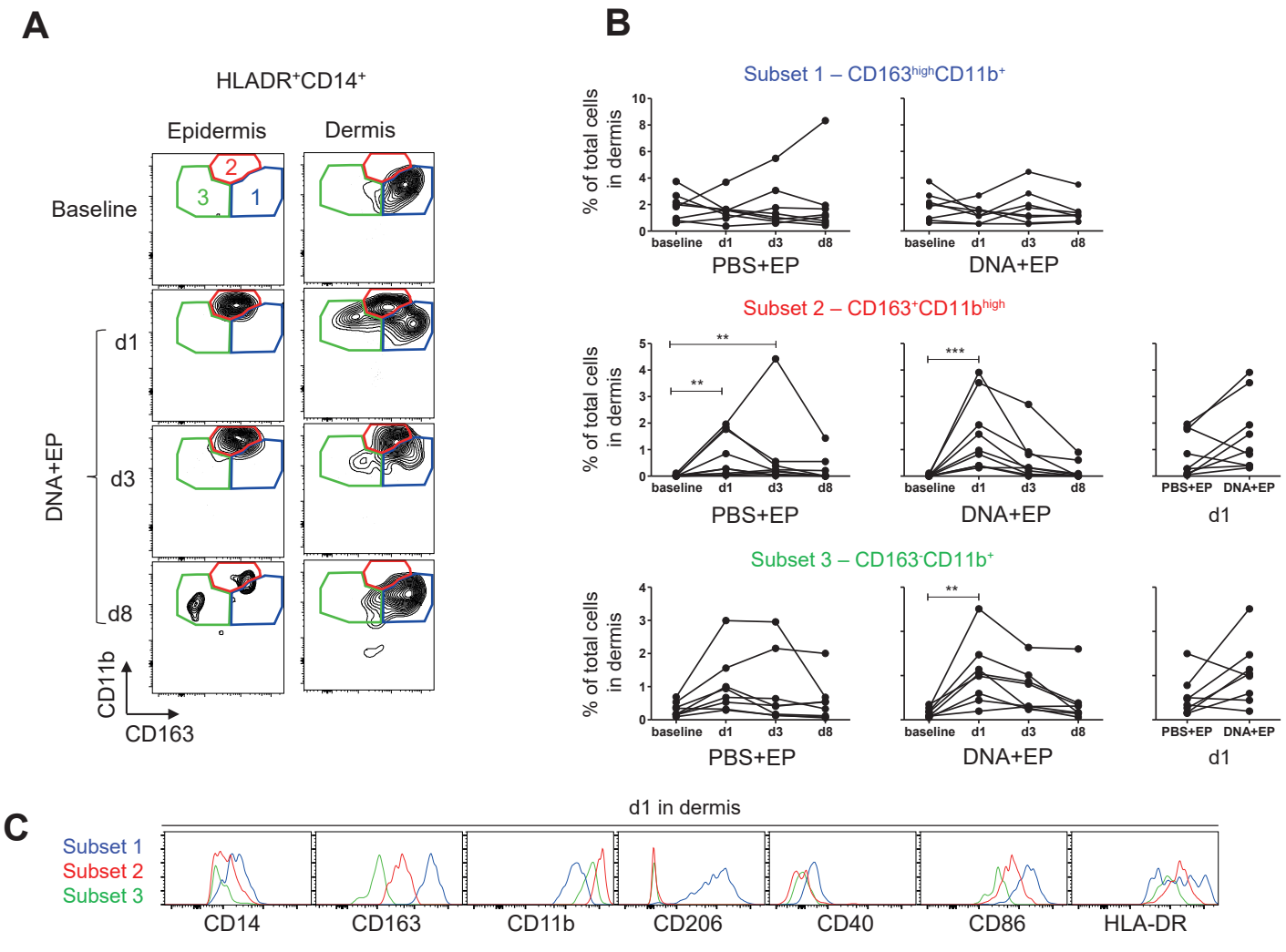
A
HLADR+CD14+
Epidermis
Dermis
Baseline
d1
d3
d8
DNA+EP
CD11b
CD163
1
2
3
B
Subset 1 – CD163highCD11b+
% of total cells in dermis
baseline d1 d3 d8
PBS+EP
DNA+EP
Subset 2 – CD163+CD11bhigh
**
***
PBS+EP DNA+EP
d1
Subset 3 – CD163-CD11b+
C
d1 in dermis
Subset 1
Subset 2
Subset 3
CD14
CD163
CD11b
CD206
CD40
CD86
HLA-DR

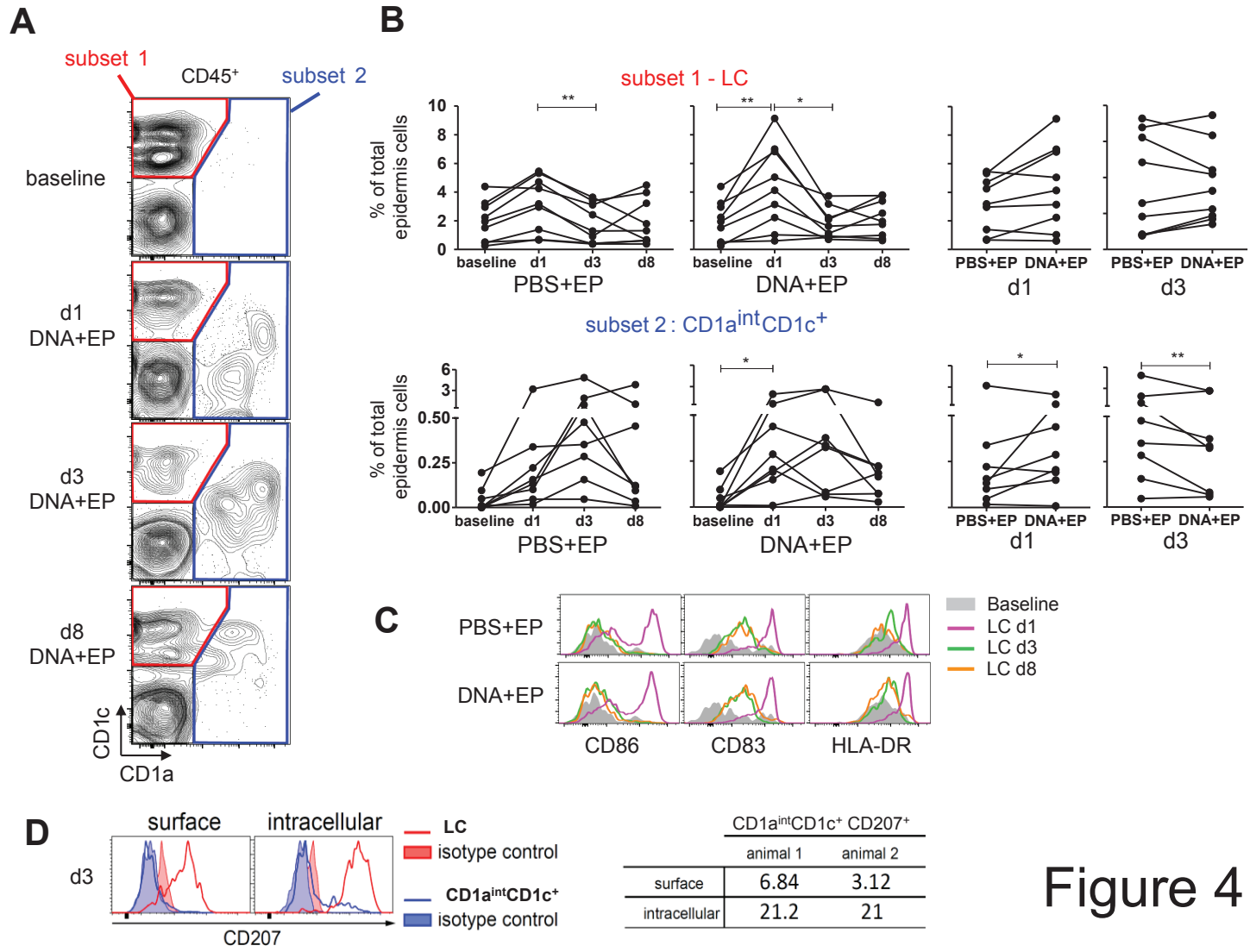

CD1a^{int}CD1c^{+} CD207^{+}	animal 1	animal 2
surface	6.84	3.12
intracellular	21.2	21

Figure 4

Figure 5

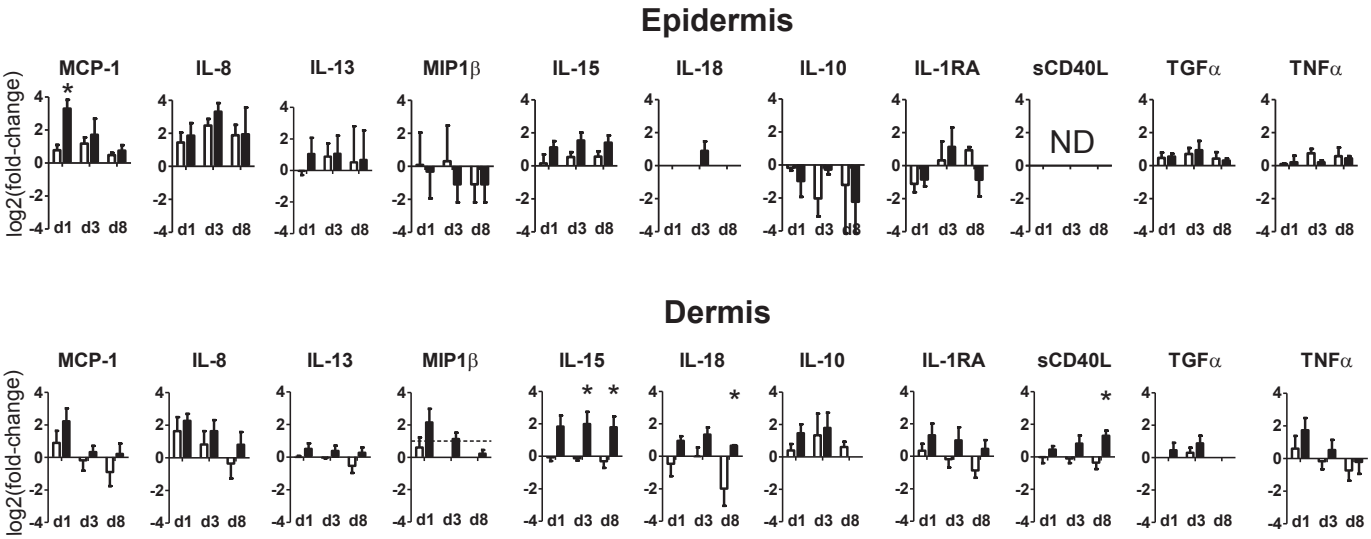
Epidermis
MCP-1
IL-8
IL-13
MIP1β
IL-15
IL-18
IL-10
IL-1RA
sCD40L
TGFα
TNFα
log2(fold-change)
ND
d1 d3 d8
Dermis
MCP-1
IL-8
IL-13
MIP1β
IL-15
IL-18
IL-10
IL-1RA
sCD40L
TGFα
TNFα
log2(fold-change)
d1 d3 d8

Figure 6

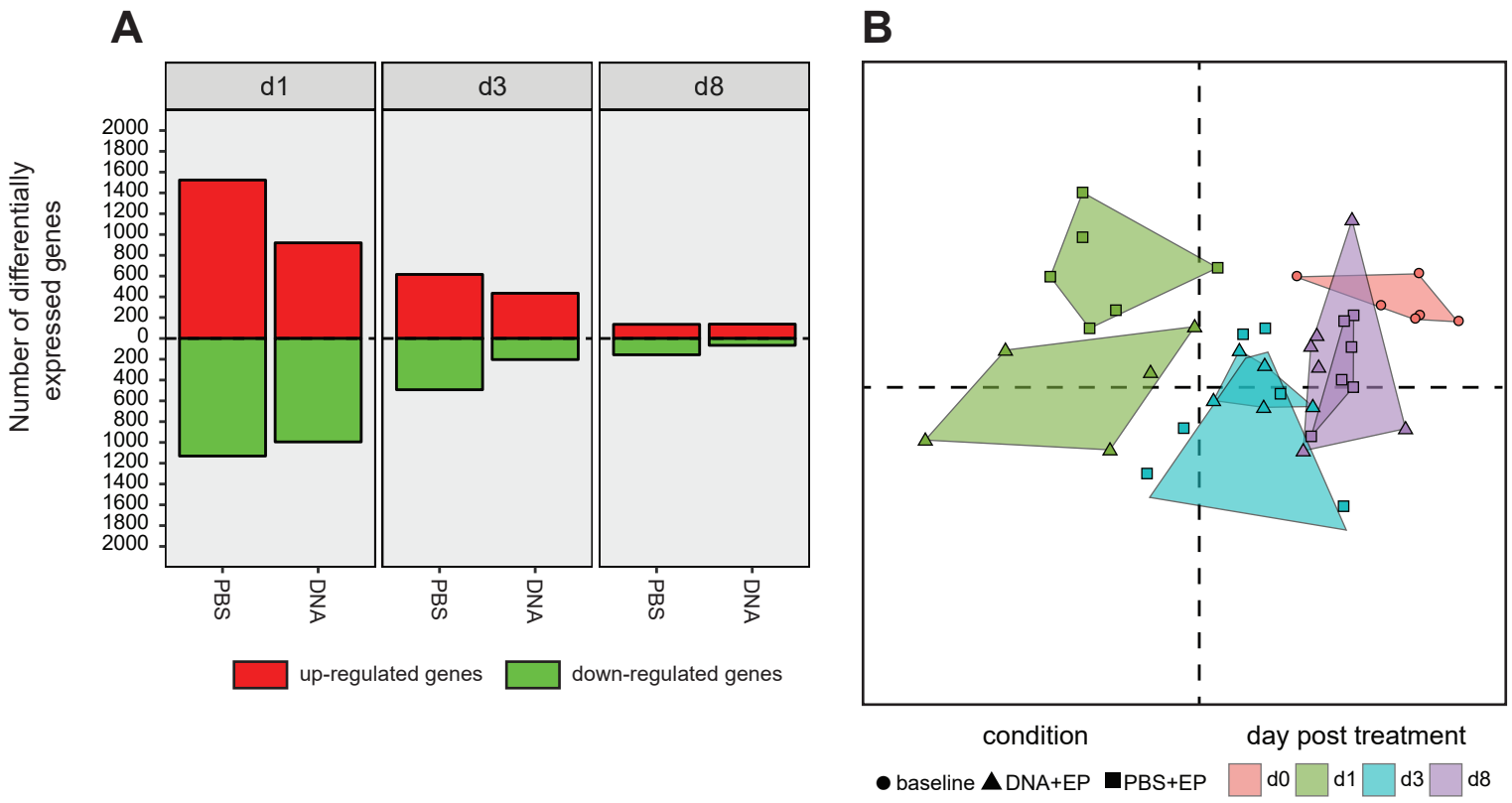
A
B
d1
d3
d8
Number of differentially expressed genes
2000
1800
1600
1400
1200
1000
800
600
400
200
0
PBS
DNA
up-regulated genes
down-regulated genes
condition
day post treatment
baseline
DNA+EP
PBS+EP
d0
d1
d3
d8

Figure 7

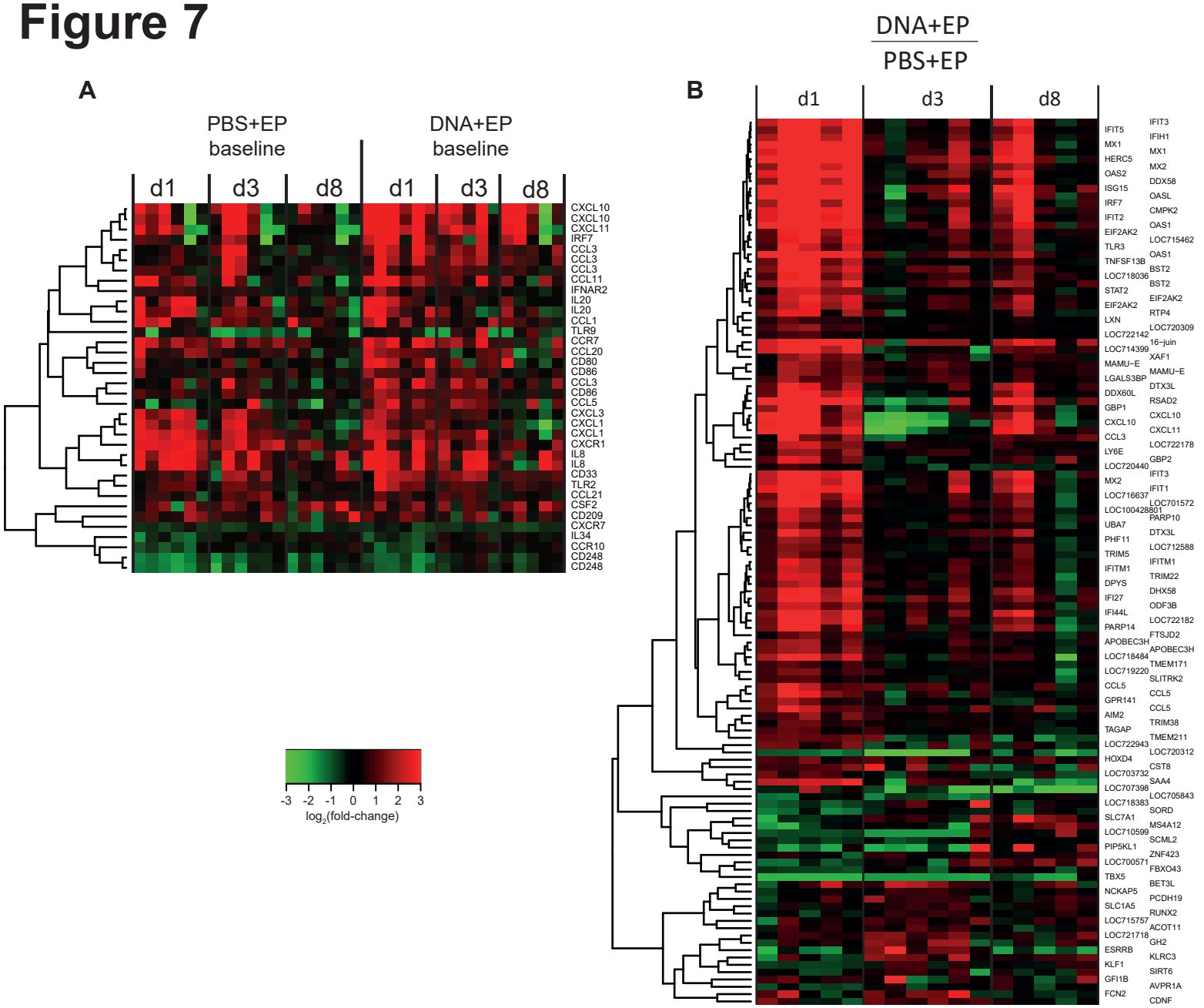
A
PBS+EP baseline
DNA+EP baseline
d1
d3
d8
d1
d3
d8
CXCL10
CXCL10
CXCL11
IRF7
CCL3
CCL3
CCL3
CCL11
IFNAR2
IL20
IL20
CCL1
TLR9
CCR7
CCL20
CD80
CD86
CCL3
CD86
CCL5
CXCL3
CXCL1
CXCL1
CXCR1
IL8
IL8
CD33
TLR2
CCL21
CSF2
CD209
CXCR7
IL34
CCR10
CD248
CD248
-3 -2 -1 0 1 2 3
log2(fold-change)
B
DNA+EP
PBS+EP
d1
d3
d8
IFIT5
MX1
HERC5
OAS2
ISG15
IRF7
IFIT2
EIF2AK2
TLR3
TNFSF13B
LOC718036
STAT2
EIF2AK2
LXN
LOC722142
LOC714399
MAMU-E
LGALS3BP
DDX60L
GBP1
CXCL10
CCL3
LY6E
LOC720440
MX2
LOC716637
LOC100428801
UBA7
PHF11
TRIM5
IFITM1
DPYS
IFI27
IFI44L
PARP14
APOBEC3H
LOC718484
LOC719220
CCL5
GPR141
AIM2
TAGAP
LOC722943
HOXD4
LOC703732
LOC707398
LOC718383
SLC7A1
LOC710599
PIP5KL1
LOC700571
TBX5
NCKAP5
SLC1A5
LOC715757
LOC721718
ESRRB
KLF1
GFI1B
FCN2
IFIT3
IFIH1
MX1
MX2
DDX58
OASL
CMPK2
OAS1
LOC715462
OAS1
BST2
BST2
EIF2AK2
RTP4
LOC720309
16-juin
XAF1
MAMU-E
DTX3L
RSAD2
CXCL10
CXCL11
LOC722178
GBP2
IFIT3
IFIT1
LOC701572
PARP10
DTX3L
LOC712588
IFITM1
TRIM22
DHX58
ODF3B
LOC722182
FTSJD2
APOBEC3H
TMEM171
SLITRK2
CCL5
CCL5
TRIM38
TMEM211
LOC720312
CST8
SAA4
LOC705843
SORD
MS4A12
SCML2
ZNF423
FBXO43
BET3L
PCDH19
RUNX2
ACOT11
GH2
KLRC3
SIRT6
AVPR1A
CDNF

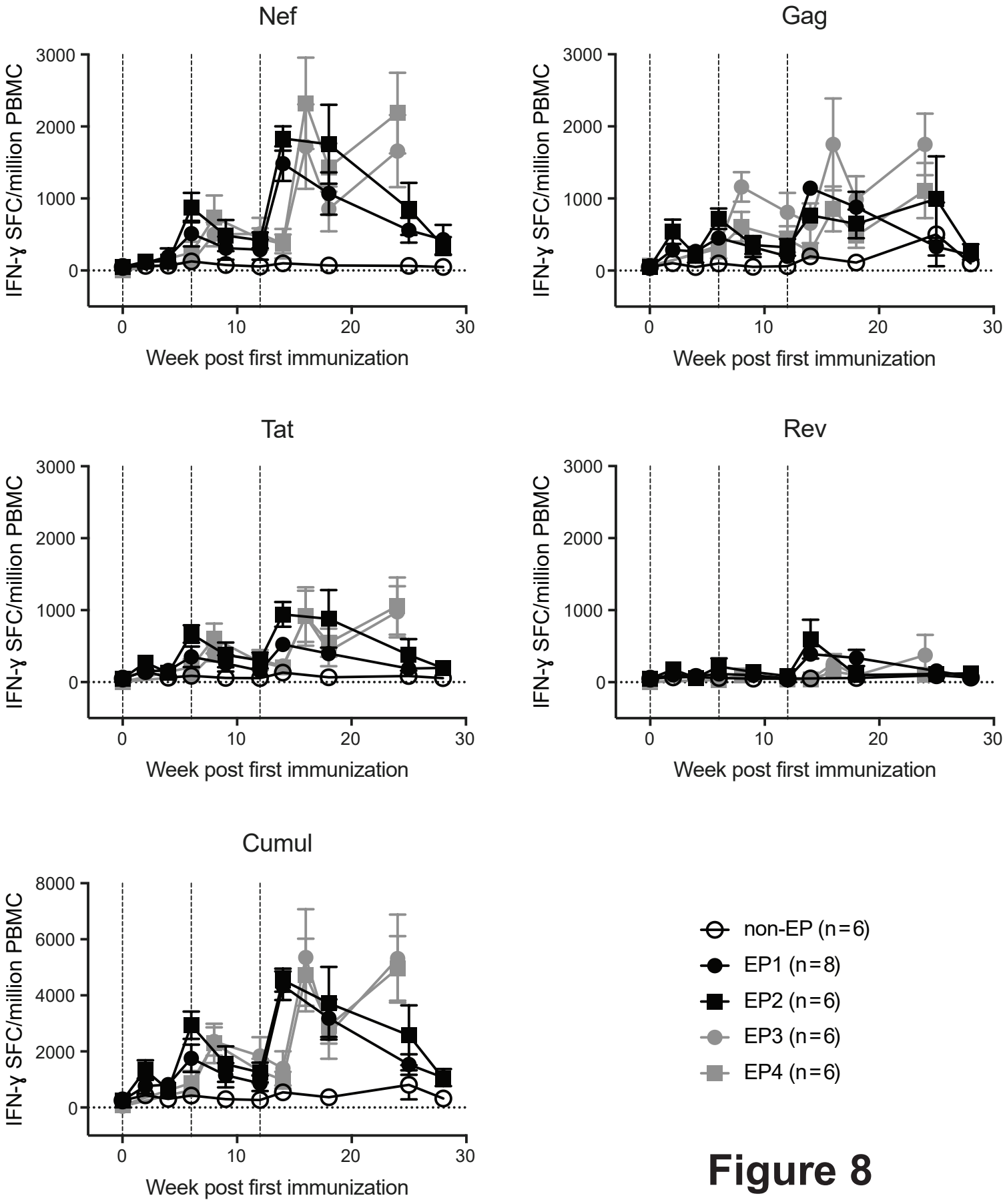
Nef
Gag
Tat
Rev
Cumul
IFN-γ SFC/million PBMC
Week post first immunization
non-EP (n=6)
EP1 (n=8)
EP2 (n=6)
EP3 (n=6)
EP4 (n=6)

Figure 8

Supplementary Material

Innate molecular and cellular signature in the skin preceding long-lasting T cell responses after electroporated auxoGTU DNA vaccination.

Lucille Adam[1], Nicolas Tchitchek[1], Biliana Todorova[1], Pierre Rosenbaum[1], Candice Poux[1], Catherine Chapon[1], Anna-Lena Spetz[2], Mart Ustav[3], Roger Le Grand[1], and Frédéric Martinon[1,*]

[1] CEA – Université Paris Sud 11 – INSERM U1184, Immunology of Viral Infections and Autoimmune Diseases, IDMIT Department, Fontenay-aux-Roses, France.

[2] Stockholm University, Department of Molecular Biosciences, The Wenner-Gren Institute, Stockholm, Sweden.

[3] Institute of Technology, University of Tartu, Tartu, Estonia.

Epidermis soluble factors	baseline	PBS+EP			DNA+EP		
		d1	d3	d8	d1	d3	d8
GM-CSF	14 ± 10	17 ± 4	18 ± 9	23 ± 13	11 ± 1	11 ± 7	15 ± 2
C-CSF	32 ± 10	12 ± 7	19 ± 21	26 ± 27	12 ± 9	22 ± 31	15 ± 10
IL-15	16.4 ± 6.7	17.7 ± 6.2	22.3 ± 4.2	23.1 ± 6.3	33.2 ± 3.2	44.2 ± 5.8	42.4 ± 16.6
IL-13	4118 ± 3296	3638 ± 2992	4759 ± 2613	4710 ± 4909	5098 ± 2485	4910 ± 1800	3968 ± 2302
IL-1RA	14 ± 7	7 ± 4	23 ± 17	26 ± 9	10 ± 7	42 ± 30	13 ± 15
IL-10	34 ± 35	27 ± 23	11 ± 9	33 ± 42	13 ± 5	23 ± 16	10 ± 9
MCP-1	3 ± 0	5 ± 2	7 ± 3	4 ± 1	33 ± 18	15 ± 17	5 ± 3
IL-8	3 ± 0	9 ± 7	16 ± 8	12 ± 8	13 ± 13	30 ± 19	33 ± 52
TGF-α	7 ± 1	10 ± 4	12 ± 4	10 ± 4	10 ± 1	15 ± 7	9 ± 2
TNF-α	17 ± 4	18 ± 4	28 ± 3	26 ± 11	19 ± 5	19 ± 5	22 ± 2
MIP-1β	28 ± 36	32 ± 43	48 ± 71	7 ± 0	17 ± 17	7 ± 0	7 ± 0
IL-2	69 ± 56	38 ± 25	40 ± 56	84 ± 84	43 ± 58	44 ± 35	25 ± 34
IL-18	ND	ND	ND	ND	ND	27 ± 19	ND
IL-12/IL-23	ND	ND	ND	ND	ND	ND	ND
MIP-1α	ND	ND	ND	ND	ND	ND	ND
IL-6	ND	ND	ND	ND	ND	ND	ND
IL-5	ND	ND	ND	ND	ND	ND	ND
IL-4	ND	ND	ND	ND	ND	ND	ND
IL-1β	ND	ND	ND	ND	ND	ND	ND
IL-17A	ND	ND	ND	ND	ND	ND	ND
sCD40L	ND	ND	ND	ND	ND	ND	ND
INFγ	ND	ND	ND	ND	ND	ND	ND

Supplementary Table 1 – Cytokines secreted in the epidermis. Cytokines secreted in the epidermis were quantified by multiplex assay at baseline at d1, d3 and d8 after PBS+EP and DNA+EP treatments (mean ± SD, n=3 per condition). Values are indicated in pg/ml, ND: cytokines production under the level of detection.

Dermis soluble factors	baseline	PBS+EP			DNA+EP		
		d1	d3	d8	d1	d3	d8
GM-CSF	3 ± 0	3 ± 1	3 ± 0	3 ± 0	5 ± 1	4 ± 3	3 ± 1
C-CSF	ND	ND	ND	ND	ND	ND	ND
IL-15	18 ± 4	17 ± 1	17 ± 1	15 ± 4	27 ± 3	30 ± 5	26 ± 3
IL-13	58 ± 22	58 ± 20	56 ± 20	38 ± 5	78 ± 14	71 ± 4	66 ± 9
IL-1RA	41 ± 21	48 ± 3	35 ± 11	21 ± 2	100 ± 42	89 ± 67	53 ± 11
IL-10	9 ± 6	15 ± 14	22 ± 16	13 ± 8	36 ± 36	31 ± 24	9 ± 6
MCP-1	43 ± 24	74 ± 38	32 ± 3	20 ± 6	183 ± 77	54 ± 36	48 ± 29
IL-8	18 ± 9	69 ± 70	29 ± 12	14 ± 7	78 ± 19	54 ± 26	33 ± 25
TGF-α	4 ± 0	4 ± 0	5 ± 2	4 ± 0	6 ± 4	8 ± 4	4 ± 0
TNF-α	9 ± 5	14 ± 10	7 ± 2	5 ± 1	27 ± 10	11 ± 2	7 ± 4
MIP-1β	ND	81 ± 64	ND	ND	279 ± 292	103 ± 41	52 ± 15
IL-2	ND	ND	ND	ND	4 ± 1	ND	ND
IL-18	5 ± 3	6 ± 5	6 ± 4	2 ± 2	10 ± 6	17 ± 15	9 ± 6
IL-12/IL-23	ND	ND	ND	ND	ND	ND	ND
MIP-1α	ND	ND	ND	ND	ND	ND	ND
IL-6	114 ± 64	96 ± 34	73 ± 51	45 ± 3	82 ± 17	57 ± 28	42 ± 7
IL-5	3 ± 1	3 ± 1	4 ± 0	2 ± 1	6 ± 0	3 ± 2	2 ± 0
IL-4	ND	ND	ND	ND	ND	ND	ND
IL-1β	ND	ND	ND	ND	6 ± 3	ND	ND
IL-17A	ND	ND	ND	ND	ND	ND	ND
sCD40L	6 ± 2	6 ± 1	6 ± 0	5 ± 2	8 ± 1	11 ± 4	15 ± 2
INFγ	ND	ND	ND	ND	ND	ND	ND

Supplementary Table 2 – Cytokines secreted in the dermis. Cytokines secreted in the dermis were quantified by multiplex assay at baseline at d1, d3 and d8 after PBS+EP and DNA+EP treatments (mean ± SD, n=3 per condition). Values are indicated in pg/ml. ND: cytokines production under the level of detection.

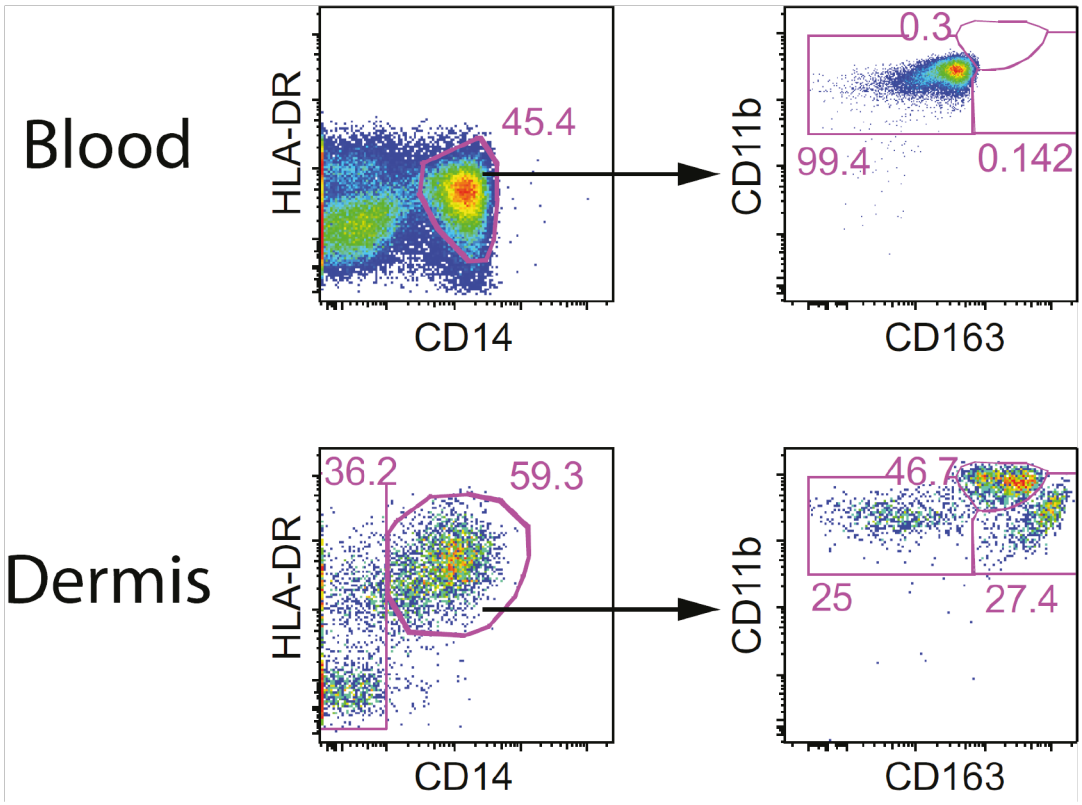

Supplementary Figure 1 – Comparison of CD14$^+$ blood monocytes and CD14$^+$ subset in dermis after DNA+EP treatment. One day after DNA+EP vaccination, three subsets of CD14$^+$ cells were observed in the dermis. The CD11b$^+$CD163$^-$subset closely resemble to CD14$^+$ blood monocytes.

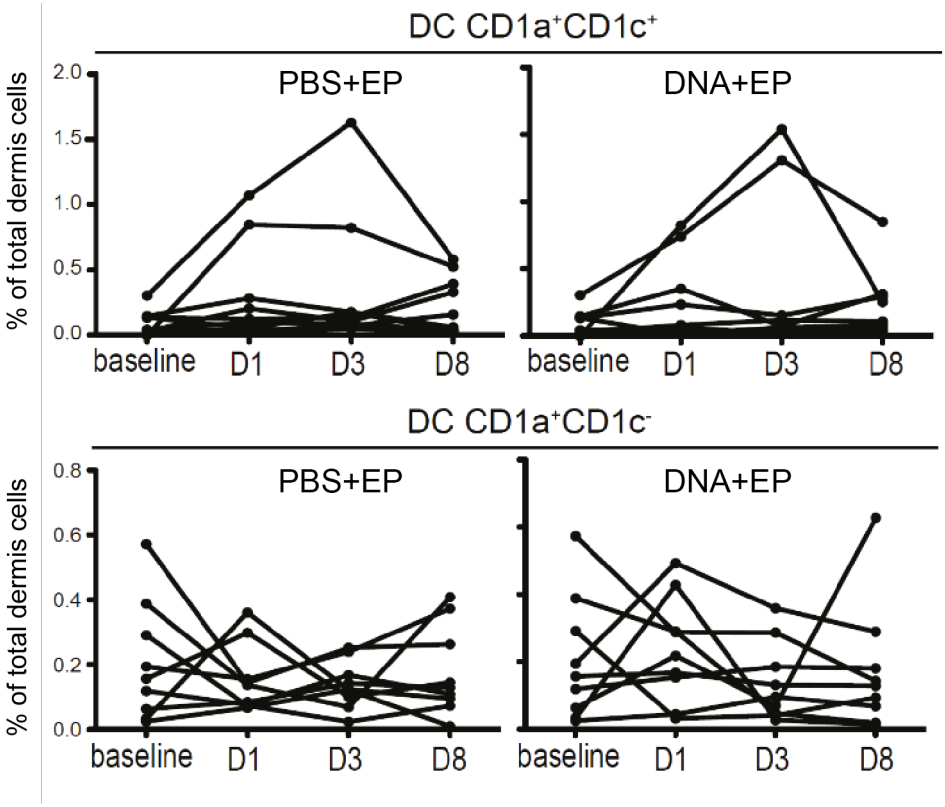

Supplementary Figure 2 – Dendritic cells subset in the dermis were not significantly modified after PBS+EP or DNA+EP treatments. Frequencies of DDC CD1a +CD1c+ and CD1a+CD1c- over time after PBS+EP and DNA+EP treatment.

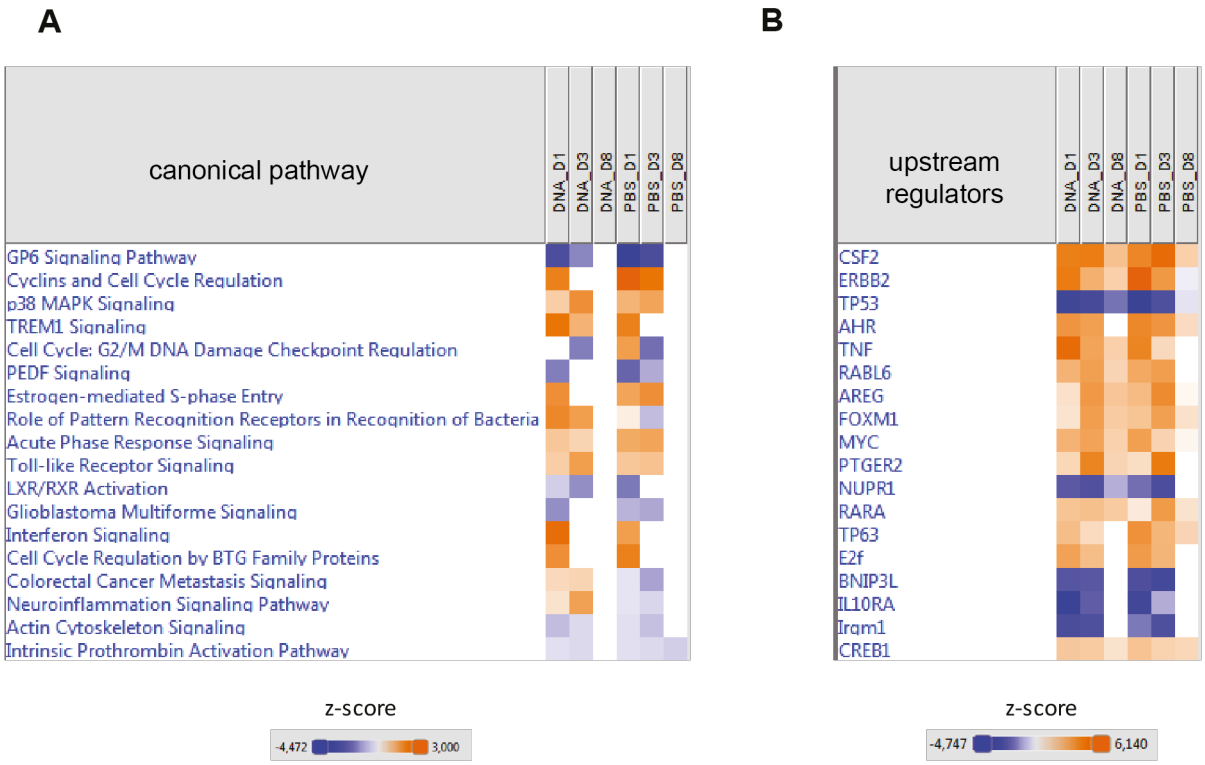

Supplementary Figure 3 – Enrichment analysis of the skin transcriptome. Heatmap representations showing the functional enrichment z-scores of Ingenuity Canonical Pathways Analysis (IPA) biological functions **(A)** and upstream regulators for each biological condition **(B)**. Each row is an IPA biological function or upstream regulators, and the columns represent the different biological conditions. The z-scores are indicated using a color gradient scale.

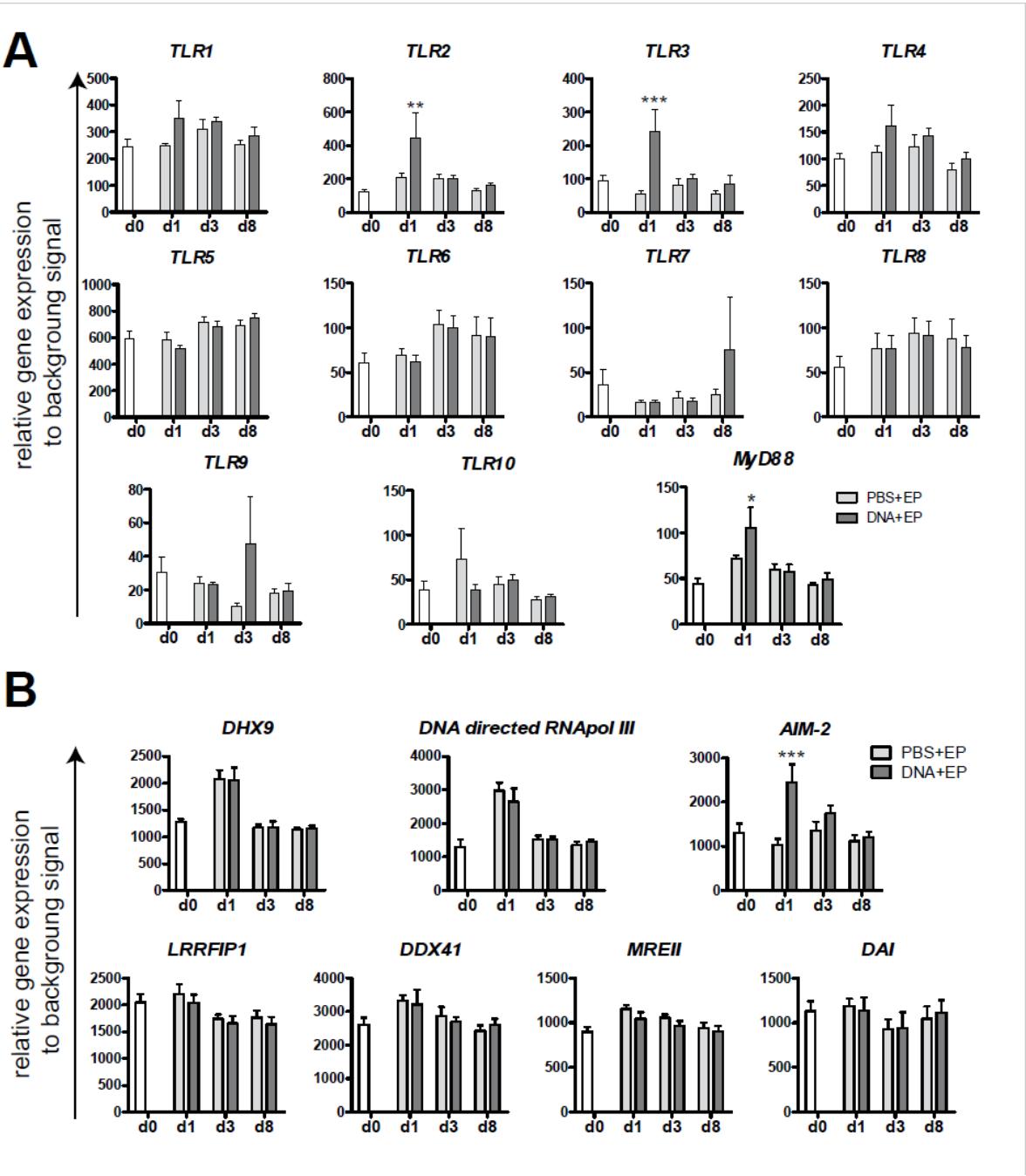

Supplementary Figure 4 – TLR and cytosolic DNA sensor regulation at the transcriptome level. Gene relative expression of skin biopsy samples collected at baseline, d1, d3 and d8 post PBS+EP and DNA+EP treatment for RNA encoding TLR (**A**) and RNA encoding cytosolic DNA sensor (**B**). **<0.05, ***<0.001.